OPTIMAL STATE-FEEDBACK AND OUTPUT-FEEDBACK CONTROLLERS FOR THE WHEELED INVERTED PENDULUM SYSTEM

A Thesis
Presented to
The Academic Faculty

by

Ashish S. Katariya

In Partial Fulfillment of the Requirements for the
Undergraduate Research Option in the
School of Electrical and Computer Engineering

School of Electrical and Computer Engineering
Georgia Institute of Technology
7 May, 2010

OPTIMAL STATE-FEEDBACK AND OUTPUT-FEEDBACK CONTROLLERS FOR THE WHEELED INVERTED PENDULUM SYSTEM

Approved by:

Professor David G. Taylor, Advisor
School of Electrical and Computer Engineering
Georgia Institute of Technology

Professor Yorai Wardi
School of Electrical and Computer Engineering
Georgia Institute of Technology

Professor Douglas B. Williams
School of Electrical and Computer Engineering
Georgia Institute of Technology

Date Approved: 7 May, 2010

To Dad, Mom, Tejhhas and Shweta

ACKNOWLEDGEMENTS

First and foremost I owe my deepest gratitude to my advisor and mentor, Prof. David G. Taylor for mentoring me and supporting me throughout my thesis for the last one year. This thesis would not have been possible unless it was for his patience, motivation, enthusiasm and immense knowledge of the subject matter. Besides my advisor, I would like to thank Prof. Yorai Wardi for agreeing to be the second reader of my thesis and thus approving it.

I would like to show my gratitude to my instructor for the thesis writing class, Prof. Jeffrey A. Donnell for giving me invaluable comments on my thesis and excellent instruction on the process of thesis writing. My sincere thanks also extends to Prof. Douglas B. Williams for helping me on various occasions with regards to completing the requirements of the Research Option.

It was an honor for me to receive the President's Undergraduate Research Award (PURA) for Fall 2009 from the Undergraduate Research Opportunities Program (UROP) office to continue my work on the thesis. I am indebted to the UROP office for also approving a Materials and Supplies Grant towards our project. I would also like to thank Mr. Andy Mastronardi, Director of Freescale University Programs for donating a Freescale MPC-555 Microcontroller Board towards our project.

Last but not the least, I am grateful to my parents for encouraging me throughout my life and eventually supporting my entire education at Georgia Tech.

TABLE OF CONTENTS

SUMMARY

Vehicles characterized as wheeled inverted pendulums have received recent attention in the robotics community. This thesis illustrates the process of designing optimal state-feedback and output-feedback controllers for the wheeled inverted pendulum system. However, since the wheeled inverted pendulum is a complex system to analyze, the cart-stick system is analyzed first. The cart-stick system is a simpler representation of the wheeled inverted pendulum system. The first step in designing a control system for any dynamic system is to derive the equations of motion or the dynamic model of the system. The exact same methodology of dynamic modeling and control system design is followed for the cart-stick system and the wheeled inverted pendulum system.

The dynamic modeling includes deriving the equations of motion using the Newtonian and Lagrangian methods, assigning appropriate state-space variables, determining the non-linear state-space model, and deriving the approximate linear model of the non-linear state-space model. The control system design includes the determination of controllability and observability, state-feedback design and output-feedback design. The optimal gain matrix for state-feedback design is determined using the Linear Quadratic Regulator (LQR) technique; whereas the optimal gain matrices for output-feedback design are determined using Loop Transfer Recovery (LTR). The results of the state-feedback and output-feedback designs are compared in the conclusions of the thesis. It is found that though output-feedback designs using an estimator hamper the performance of a system, it is necessary to consider and prototype output-feedback control systems because all state variables are almost never available for full-state feedback.

CHAPTER I

INTRODUCTION

1.1 The Wheeled Inverted Pendulum System

In recent years, the usage of industrial robots by manufacturing companies has increased drastically but there hasn't been much progress in the usage of mobile robots in human environments. The human-machine interface is a key area of interest, particularly in the physical interaction between the robot and person. However, robotic arms and mobile robots used in industries are heavy and occupy much space i.e. they are position-controlled rather than force-controlled [1]. These heavy industrial robots cannot be accommodated in an environment occupied by humans due to their lack of dynamic agility. Therefore, it becomes necessary to build intelligent robots with dynamic stability that are safe, agile, and easy to maneuver in communities and building spaces occupied by humans [1].

Figure 1: The Segway Personal Transporter.

One such system that can easily maneuver in a crowded environment is the wheeled inverted pendulum system. Vehicles characterized as wheeled inverted pendulums have received recent attention in the robotics community [2]. A wheeled inverted

pendulum is a body above two wheels with no balancing support. A commercial version of the wheeled inverted pendulum, the Segway Personal Transporter, shown in Figure 1 has inspired the interest of many researchers. Due to the inherent non-linearities and complex dynamics of the wheeled inverted pendulum system, the control of this system becomes a challenging problem. This thesis will illustrate the process of designing optimal state-feedback and output-feedback controllers for the wheeled inverted pendulum system.

1.2 Literature Review

A wheeled inverted pendulum is a non-linear system which can be controlled by a digital controller. Though the control system feedback loop can be linear, all non-linearities of the plant should be maintained in the simulation model of the plant in order to obtain accurate predictions of control performance through simulation. However, most of previous works [2], [3], [4] and [5] failed to perform simulations capable of investigating the role of plant nonlinearity on closed-loop system stability and performance. Owing to the interest of various researchers, [3] was one of the first papers to discuss the control system design of the wheeled inverted pendulum system. A 3D model of the wheeled inverted pendulum system from [3] is shown in Figure 2.

One of the most important steps in designing a control system is to do the dynamic modeling correctly. The two most common approaches used for deriving the equations of motion of a dynamic system are the Newtonian and Lagrangian approaches. To ensure the validity of the derived equations of motion, these equations should be cross-checked using both methods. Equations from both methods should be exactly the same [6]. However, none of the previous works [2], [3], [4], [5] and [7] that design a control system for the wheeled inverted pendulum system derive the equations of motion using two approaches. Hence, the validity of the derived equations of motion in some papers is questionable.

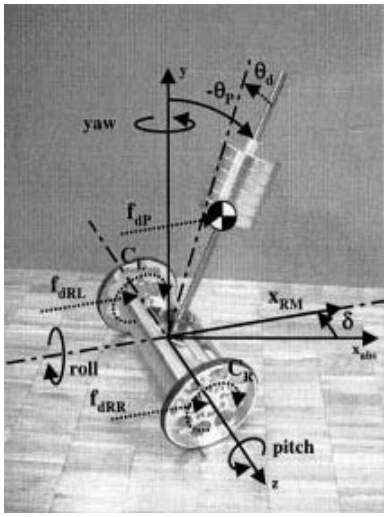

Figure 2: JOE: A Mobile, Inverted Pendulum [3].

In the state-space design method for control systems, the two ways of designing a control system are state-feedback and output-feedback. While state-feedback assumes that all state variables are at our disposal [8], output-feedback considers sensor selection and is a more realistic approach towards control system design because usually, not all state variables are available for measurement. However, very few papers in the past have extensively covered output-feedback control system design for the wheeled inverted pendulum system. Also, most papers that have considered state-feedback or output-feedback designs have determined the gain matrices through manual pole placement. Although manual pole placement provides satisfactory control, it does not provide optimal control.

All the above shortcomings in previous research related to the wheeled inverted pendulum system will be eliminated in this thesis. Firstly, all non-linearities are included in the simulation model of the plant for the purpose of assessing the stability and performance of the control system design. Secondly, the dynamic model of the wheeled inverted pendulum system will be determined using both, the Newtonian and Lagrangian approaches to ensure the validity of the derived equations. Lastly, both state-feedback and output-feedback controllers will be designed for the wheeled

inverted pendulum system. The gain matrices will be determined using optimal control techniques such as Linear Quadratic Regulator (LQR) and Loop Transfer Recovery (LTR).

1.3 Thesis Outline

As mentioned earlier, this thesis will illustrate the process of designing optimal state-feedback and output-feedback controllers for the wheeled inverted pendulum system. However, since the wheeled inverted pendulum is a complex system to analyze, the cart-stick system will be analyzed first. The cart-stick system is a simpler representation of the wheeled inverted pendulum system. The first step in designing a control system for any dynamic system is to derive the equations of motion or the dynamic model of the system. The exact same methodology of dynamic modeling and control system design will be followed for the cart-stick system and the wheeled inverted pendulum system.

The dynamic modeling will include deriving the equations of motion using the Newtonian and Lagrangian methods, assigning appropriate state-space variables, determining the non-linear state-space model, and deriving the approximate linear model of the non-linear state-space model. The control system design will include the determination of controllability and observability, state-feedback design and output-feedback design. The optimal gain matrix for state-feedback design will be determined using the LQR technique; whereas the optimal gain matrices for output-feedback design will be determined using LTR. The results of the state-feedback and output-feedback designs will be compared in the conclusions of the thesis.

CHAPTER II

CART-STICK SYSTEM

The cart-stick system consists of an inverted pendulum and a cart. The pivot point of the inverted pendulum is mounted on a cart that can move horizontally. The cart-stick system may also be called a cart-pole system sometimes. A schematic diagram of the cart-stick system is shown in Figure 3. Since the system has inherent non-linearities and instability, it needs to be controlled by applying a torque to the cart's wheels and thus balancing the stick upright.

Now, the cart has four wheels and to be able to move the cart horizontally, at least two wheels on the same axle need to be torque actuated. Introducing wheel dynamics for actuating torques will unnecessarily complicate the system. Instead, considering a fictitious horizontal force on the cart is equivalent to actuating torques on the wheels since both will be used to move the cart horizontally. Also, for reasons of simplicity, a point mass instead of distributed mass will be considered for the inverted pendulum on the cart-stick system. It should be kept in mind that our eventual goal is to prototype the wheeled inverted pendulum system and not the cart-stick system. Thus, these simplifications of using a fictitious horizontal force and point mass will be removed while analyzing the wheeled inverted pendulum system in Chapter 3.

One can note that the cart-stick system has only two degrees of freedom i.e. translation along the X axis and rotation of the stick about the pivot point. Whereas, the wheeled inverted pendulum system, as we will learn in Chapter 3, has three degrees of freedom i.e. translation along the X axis, rotation about the pitch axis and rotation about the yaw axis. The pitch and yaw axes will be explained in further detail in Chapter 3. It should be quite apparent by now that the cart-stick system is

a simpler representation of the wheeled inverted pendulum system and thus it would be beneficial to analyze the cart-stick system first before moving on to the wheeled inverted pendulum system.

The first step in designing a control system for the cart-stick system is to derive the equations of motion. This chapter will outline the dynamic modeling of the cart-stick system and the design of controllers for the same. As mentioned earlier in the thesis outline, the dynamic modeling will include deriving the equations of motion using the Newtonian and Lagrangian methods, assigning appropriate state-space variables, determining the non-linear state-space model, and deriving the approximate linear model of the non-linear state-space model. The control system design will include the determination of controllability and observability, state-feedback design and output-feedback design.

2.1 Dynamic Modeling of the Cart-Stick System

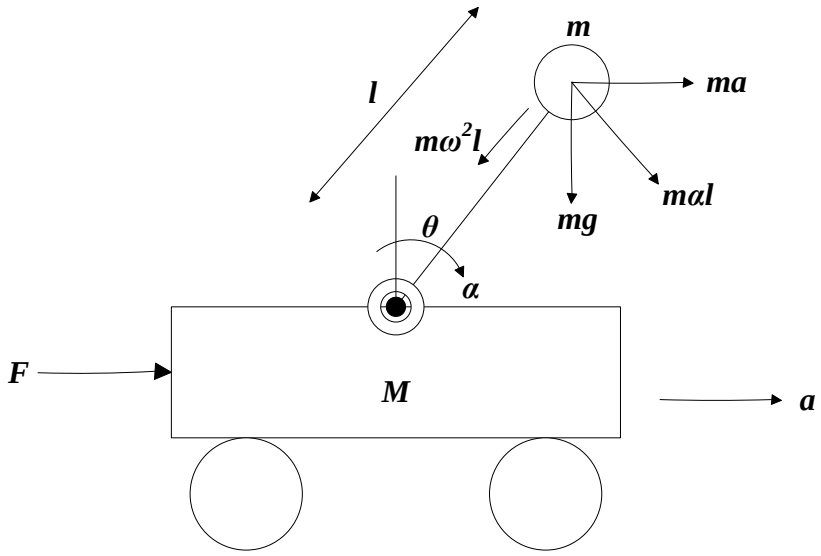

Figure 3: Schematic of the cart-stick system with all relevant forces and accelerations labeled.

As mentioned earlier, the mathematical model of the cart-stick system will be derived using the Newtonian and Lagrangian approaches. It can be verified that the

equations obtained from both methods are exactly the same; thus, deriving the equations of motion using two methods warrants the validity of the derived mathematical model. It is assumed for both approaches that the right-hand side direction is the $+x$ direction, the upward direction is the $+y$ direction and a clockwise sense is a $+ve$ rotation. Refer to the schematic diagram of the cart-stick system shown in Figure 3 for the assumed forces and accelerations. A list of variables used in the dynamic modeling of the cart-stick system is given in Section A.1 of Appendix A.

2.1.1 Newtonian Approach

Using Newton's second law motion is one of the most common methods to derive the equations of motion of a dynamic system. Thus, applying $\sum F = Ma$ on the cart and stick separately, we get

$$F + N = Ma \quad \text{and} \quad N = m\omega^2 l \sin\theta - ma - m\alpha l \cos\theta$$

respectively. The horizontal relation force between the cart and the stick, N needs to be eliminated and thus, simplifying the above equations, we find

$$F = (m + M)a - m\omega^2 l \sin\theta + m\alpha l \cos\theta \tag{1}$$

Now, the total external torque acting on the mass m about the point of contact between the cart and stick is $mgl \sin\theta$ and the moment of inertia of m about the same point is ml^2. Hence, applying $\sum \tau = I\alpha$ about this point of contact, we find

$$mgl \sin\theta = ml^2(\alpha + a \cos\theta)$$

$$\Rightarrow mg \sin\theta = m\alpha l + mal \cos\theta$$

$$\Rightarrow g \sin\theta - \alpha l - a \cos\theta = 0 \tag{2}$$

Equations (1) and (2) are sufficient to describe the dynamics of the cart-stick system since only two equations are needed to solve for the unknowns a and α. Also, the internal relation force, N has been eliminated.

2.1.2 Lagrangian Approach

Another way to derive the equations of motion of dynamic systems is the Lagrangian approach. The Lagrangian method allows one to deal with scalar energy functions rather than vector forces and accelerations as in the Newtonian method, thus reducing the chances of error. Also, in many complex cases like the wheeled inverted pendulum system, the Lagrangian approach turns out to be simpler than the Newtonian approach.

Now, for the cart-stick system, the variables (describing the motion and system parameters) used for Lagrangian approach are the same as those used for the Newtonian approach, except that some variables such as the relation forces between the cart and stick will not be needed for the Lagrangian approach. The first step in deriving the equations of motion using the Lagrangian method is to derive the Lagrangian $\mathcal{L}$;

$$\mathcal{L} = T - V$$

where T and V are the total kinetic and potential energies of the system respectively.

Let us start by finding the total kinetic energy of the system at any given time. The X and Y co-ordinates of m at any given time would be $(x + l\sin\theta)$ and $(l\cos\theta)$ respectively. The X and Y components of the velocity of m can be obtained by differentiating the position co-ordinates of m. Therefore, $v_x = (\dot{x} + l\dot{\theta}\cos\theta)$ and $v_y = (-l\dot{\theta}\sin\theta)$. Hence, the total kinetic energy of the system, T can be written as

$$T = \frac{1}{2}M\dot{x}^2 + \frac{1}{2}m[(\dot{x} + l\dot{\theta}\cos\theta)^2 + (-l\dot{\theta}\sin\theta)^2] \tag{3}$$

Considering the cart to be at ground reference level and m to be the only mass above this reference level, the total potential energy of the system, V can be written as

$$V = mgl\cos\theta \tag{4}$$

Equations (3) and (4) can then be used to find the Lagrangian,

$$\mathcal{L} = \frac{1}{2}(M+m)\dot{x}^2 + ml\dot{x}\dot{\theta}\cos\theta + \frac{1}{2}ml^2\dot{\theta}^2 - mgl\cos\theta \tag{5}$$

Recall that the cart-stick system has two degrees of freedom and F is the only external force applied to the system that is capable of changing x or $\dot{x}$. However, no external force or torque applied to the system affects θ directly. Hence, the equations of motion for the cart-stick system will be derived by simplifying

$$\frac{d}{dt}\frac{\partial \mathcal{L}}{\partial \dot{x}} - \frac{\partial \mathcal{L}}{\partial x} = F \quad \text{and} \quad \frac{d}{dt}\frac{\partial \mathcal{L}}{\partial \dot{\theta}} - \frac{\partial \mathcal{L}}{\partial \theta} = 0$$

The first equation of motion can be found by simplifying

$$\frac{d}{dt}\frac{\partial \mathcal{L}}{\partial \dot{x}} - \frac{\partial \mathcal{L}}{\partial x} = F \tag{6}$$

$$\Rightarrow \frac{d}{dt}[(M+m)\dot{x} + ml\dot{\theta}\cos\theta] = F$$

$$\Rightarrow (M+m)\ddot{x} + ml\ddot{\theta}\cos\theta - ml\dot{\theta}^2\sin\theta = F$$

$$\Rightarrow F = (m+M)a - m\omega^2 l\sin\theta + m\alpha l\cos\theta \tag{7}$$

Similarly, the second equation of motion can be found by simplifying

$$\frac{d}{dt}\frac{\partial \mathcal{L}}{\partial \dot{\theta}} - \frac{\partial \mathcal{L}}{\partial \theta} = 0 \tag{8}$$

$$\Rightarrow \frac{d}{dt}[ml\dot{x}\cos\theta + ml^2\dot{\theta}] - [-ml\dot{x}\dot{\theta}\sin\theta + mgl\sin\theta] = 0$$

$$\Rightarrow ml(\ddot{x}\cos\theta - \dot{x}\dot{\theta}\sin\theta + l\ddot{\theta} + \dot{x}\dot{\theta}\sin\theta - g\sin\theta) = 0$$

$$\Rightarrow g\sin\theta - \alpha l - a\cos\theta = 0 \tag{9}$$

It can be seen that (1) and (2) are exactly the same as (7) and (9) respectively. This verification signifies that the dynamic modeling of the cart-stick system has been done correctly and that these equations are sufficient to describe the dynamics of the cart-stick system.

2.1.3 State Assignment and Non-Linear Model

Equations (7) and (9) are not explicitly defined in terms of a and α and hence need to be solved simultaneously. Further solving (7) and (9) simultaneously to derive a and α explicitly, we find that

$$a = \frac{m\omega^2 l \sin\theta - mg \sin\theta \cos\theta + F}{m \sin^2\theta + M}$$

$$\alpha = \frac{(m+M)g \sin\theta - m\omega^2 l \sin\theta \cos\theta - F\cos\theta}{Ml + ml \sin^2\theta}$$

The general form of a state-space model for non-linear systems is given by

$$\dot{x} = f(x, u) \tag{10}$$

where x is a vector of state variables and u is system control input F. The state variable assignment for the cart-stick system is done as

$x_1(t) = x =$ X co-ordinate of the cart

$x_2(t) = v =$ Translational velocity of the cart in the X direction

$x_3(t) = \theta =$ Vertical angle of the stick w.r.t the Y axis

$x_4(t) = \omega =$ Angular velocity of the stick

$u(t) = F =$ Linear external force applied on the cart in the $+x$ direction

Hence, the model equations are written in state space form as

$$\begin{aligned}
\dot{x}_1(t) &= x_2(t) \\
\dot{x}_2(t) &= \frac{mlx_4^2(t)\sin x_3(t) - mg \sin x_3(t)\cos x_3(t) + u(t)}{M + m\sin^2 x_3(t)} \\
\dot{x}_3(t) &= x_4(t) \\
\dot{x}_4(t) &= \frac{-mlx_4^2(t)\sin x_3(t)\cos x_3(t) + (M+m)g\sin x_3(t) - u(t)\cos x_3(t)}{Ml + ml\sin^2 x_3(t)}
\end{aligned}$$

2.1.4 Linear Model

Linearization is the process of finding a linear model that approximates a non-linear one [11]. The linear state space model of the aforementioned non-linear model

needs to be derived so that tests of controllability and observability can be performed on the model. The first step in deriving the linear approximate model is to determine the equilibrium points associated with stationary balancing. The equilibrium points are denoted by $(\bar{x}, \bar{u})$ where $\bar{x}$ is a vector of the state variables x_1 through x_4 and $\bar{u}$ is the linear force input F. The equilibrium points $(\bar{x}, \bar{u})$ satisfy

$$0 = f(\bar{x}, \bar{u}) \tag{11}$$

where the above equation denotes the non-linear state space model derived in Section 2.1.3. The non-linear model can be rewritten using (11) as

$$\begin{aligned}
0 &= \bar{x}_2 \\
0 &= \frac{ml\bar{x}_4^2 \sin \bar{x}_3 - mg \sin \bar{x}_3 \cos \bar{x}_3 + \bar{u}}{M + m \sin^2 \bar{x}_3} \\
0 &= \bar{x}_4 \\
0 &= \frac{-ml\bar{x}_4^2 \sin \bar{x}_3 \cos \bar{x}_3 + (M+m)g \sin \bar{x}_3 - \bar{u} \cos \bar{x}_3}{Ml + ml \sin^2 \bar{x}_3}
\end{aligned}$$

$$\Rightarrow \quad \bar{x}_1 = \bar{x}_2 = \bar{x}_4 = 0$$

The remaining equations are

$$-mg \sin \bar{x}_3 \cos \bar{x}_3 + \bar{u} = 0 \tag{12}$$

$$(M+m)g \sin \bar{x}_3 - \bar{u} \cos \bar{x}_3 = 0 \tag{13}$$

Now, there are two unknowns in (12) and (13), namely $\bar{x}_3$ and $\bar{u}$ which need to be solved for. Distinct real solutions for $\bar{x}_3$ and $\bar{u}$ satisfying these equations are

$$\bar{x}_3 = 0 \quad , \quad \bar{u} = 0 \tag{14}$$

$$\bar{x}_3 = \pm\pi \quad , \quad \bar{u} = 0 \tag{15}$$

However, solution (15) is not a valid equilibrium point for this particular cart-stick system because $\bar{x}_3 = \pm\pi$ would mean that the vertical angle is $\pm 180^\circ$ with respect to

the $+y$ direction. This solution would signify that the stick of the cart-stick system runs into the ground to achieve equilibrium; however, this is physically not possible. It follows that the only equilibrium point for the cart-stick system is

$$\bar{x} = \begin{bmatrix} \bar{x}_1 \\ \bar{x}_2 \\ \bar{x}_3 \\ \bar{x}_4 \end{bmatrix} = \begin{bmatrix} 0 \\ 0 \\ 0 \\ 0 \end{bmatrix} \quad , \quad \bar{u} = 0 \tag{16}$$

One can compute a linear model that is valid for small signals, for a system with smooth non-linearities and a continuous derivative. Hence, the linear model equations can be derived in the form

$$\dot{x} = Ax + Bu \tag{17}$$

from the general non-linear form

$$\dot{x} = f(x, u)$$

where,

$$A = \begin{bmatrix} \frac{\partial f_1}{\partial x_1} & \cdots & \frac{\partial f_1}{\partial x_4} \\ \vdots & \ddots & \vdots \\ \frac{\partial f_4}{\partial x_1} & \cdots & \frac{\partial f_4}{\partial x_4} \end{bmatrix}_{\bar{x},\bar{u}} \quad \text{and} \quad B = \begin{bmatrix} \frac{\partial f_1}{\partial u} \\ \vdots \\ \frac{\partial f_4}{\partial u} \end{bmatrix}_{\bar{x},\bar{u}}$$

Solving for A and B, and substituting the values for $\bar{x}$ and $\bar{u}$ from (16), the two matrices can be written as

$$A = \begin{bmatrix} 0 & 1 & 0 & 0 \\ 0 & 0 & -\frac{mg}{M} & 0 \\ 0 & 0 & 0 & 1 \\ 0 & 0 & \frac{(m+M)g}{Ml} & 0 \end{bmatrix} \quad \text{and} \quad B = \begin{bmatrix} 0 \\ \frac{1}{M} \\ 0 \\ -\frac{1}{Ml} \end{bmatrix} \tag{18}$$

Hence, the linear model for the wheeled inverted pendulum is given by

$$\dot{x} = \begin{bmatrix} \dot{x_1} \\ \dot{x_2} \\ \dot{x_3} \\ \dot{x_4} \end{bmatrix} = \begin{bmatrix} 0 & 1 & 0 & 0 \\ 0 & 0 & -\frac{mg}{M} & 0 \\ 0 & 0 & 0 & 1 \\ 0 & 0 & \frac{(m+M)g}{Ml} & 0 \end{bmatrix} \begin{bmatrix} x_1 \\ x_2 \\ x_3 \\ x_4 \end{bmatrix} + \begin{bmatrix} 0 \\ \frac{1}{M} \\ 0 \\ -\frac{1}{Ml} \end{bmatrix} \begin{bmatrix} F \end{bmatrix} \tag{19}$$

2.2 Control System Design

In feedback control systems, the variable being controlled—such as vertical angle of the stick—is either measured by a sensor or estimated, and the measured or estimated information is fed back to the controller to influence the controlled variable. The central component of any feedback system is the *process* whose output is to be controlled. In our system, the process is the cart and stick whose outputs are the state variables x_1 through x_4. The *actuator* is a device that can influence the controlled variable of the process. In our system, the actuator is a fictitious device that produces a linear horizontal force, F applied on the cart. The combination of process and actuator is called the *plant*, and the component that actually computes the desired control signal is the *controller* [8].

Like any other dynamic system, there are two ways of designing a feedback control system for the cart-stick system using the state-space design method. The first approach, *state-feedback* involves finding the control law as feedback of a linear combination of the state variables [8]. In state-feedback design, it is assumed that all elements of the state vector are at our disposal. This design method is sometimes also called full-state feedback. Also, to be able to design a state-feedback system, it is sufficient that the system is *controllable*. It should be noted that, *controllability* is an inherent property of the plant with actuators already in place while assuming that all state variables are available for measurement and without considering appropriate sensor selection.

However, for a real-world system, assuming that all state variables and so many sensors are available for measurement would be an invalid assumption. Hence, the second approach, *output-feedback* is necessary if full-state feedback is not available. An output-feedback design making the use of an estimator computes an estimate of the entire state vector when provided with the measurements of certain system parameters using a limited selection of sensors. An estimator is sometimes also called an *observer*. Analogous to state-feedback design, to be able to design an output-feedback system, it is sufficient that the system is *observable*. It should be noted that, *observability* is a property of the plant with appropriate sensor selection without considering actuator selection.

Thus, we will first determine the controllability of the cart-stick system and then design a state-feedback control system. We will then determine the observability of the cart-stick system and design an output-feedback control system for the same.

2.2.1 Cart-Stick System Physical Parameters

For simulation purposes, actual values for physical parameters of the cart-stick system need to be used. These values are chosen such that it is actually possible to build this cart-stick system. The physical parameter values used in simulations are

m	(mass of the stick)	$=$	5	kg
M	(mass of the cart)	$=$	20	kg
l	(length of the stick)	$=$	0.4	m
g	(acceleration due to gravity)	$=$	9.81	$\mathrm{m/s^2}$

2.2.2 Controllability of Cart-Stick System

The system (A, B) is *controllable* if there exists a (piecewise continuous) control signal $u(t)$ that will take the state of the system from any initial state x_i to any desired final state x_f in a finite time interval [11]. Mathematically, the algebraic

controllability theorem states that (A, B) is controllable if and only if

$$\text{rank}\begin{bmatrix} B & AB & \cdots & A^{n-1}B \end{bmatrix} = n = \dim(x) \tag{20}$$

where the matrices A and B are from the linear model of the cart-stick system given in (18). Since, there are four state variables in the state-space model of the cart-stick system, $n = \dim(x) = 4$. The rank of the controllability matrix

$$\begin{bmatrix} B & AB & A^2B & A^3B \end{bmatrix}$$

is determined to be 4 using the Matlab script given in Section B.1 of Appendix B. Since, the controllability test given in (20) is satisfied, the system is controllable. The cart-stick system can thus be successfully controlled using a state-feedback control system.

2.2.3 State-Feedback Control System Design

The design of a *state-feedback* control system providing full-state feedback is given by

$$\begin{aligned} \text{Plant:} \quad \dot{x}(t) &= f(x(t), u(t)) \\ \text{State-feedback:} \quad u(t) &= -Kx(t) \end{aligned}$$

where state-feedback, the control law as feedback of a linear combination of the state variables is

$$u = -Kx = -\begin{bmatrix} K_1 & K_2 & \cdots & K_n \end{bmatrix} \begin{bmatrix} x_1 \\ x_2 \\ \vdots \\ x_n \end{bmatrix}$$

In the above equation, K is said to be the *gain matrix* and for an nth-order system, there will be n feedback gains, $K_1, \ldots, K_n$. For the cart-stick system, $n = 4$ since there are four state variables. It should be noted that inherent non-linearities of the cart-stick system are maintained in the simulation model by using non-linear equations

for $\dot{x}(t)$ from Section 2.1.3. However, a linear design model is used to determine the gain matrix, K.

Now, perhaps the most important step in designing a regulator using the state-space design method is to determine the gain matrix, K. One common approach to determine K is to assign a set of pole locations for the closed-loop system that will correspond to satisfactory dynamic response in terms of control effort and other measures of transient response. After assigning the pole locations, the Matlab command `place` can be used to determine K. However, the gain matrix K determined by manually assigning pole locations provides satisfactory control, not optimal control.

Another effective and widely used technique of linear control systems design is the optimal *Linear Quadratic Regulator* (LQR). The central idea behind the theory of optimal control, including LQR design, is to control a dynamic system at minimum cost. Now, consider a continuous-time linear system described by

$$\begin{aligned} \dot{x} &= Ax + Bu \\ y &= Cx \end{aligned}$$

where y is the output of the system and C is the output matrix. Usually, y is a vector of sensor measurements and the number of elements in y is equal to the number of sensors being used. After y has been determined by appropriate sensor selection, the output matrix C is determined accordingly. However, since we are designing a state-feedback system while keeping in mind that all state variables are available for measurement, y can consist of all four state variables and C can thus be an identity matrix.

Coming back to LQR design, the performance index, $\mathcal{J}$ that needs to be minimized for the linear system described above is given by

$$\mathcal{J} = \int_0^\infty (x^T Q x + u^T R u) dt \tag{21}$$

where x is a vector of state variables, u is a vector of system inputs, and Q and R are weighting matrices chosen by the designer [8]. The matrices Q and R signify the trade-off between performance and control effort respectively. It should be noted that the control law that minimizes $\mathcal{J}$ is given by linear state-feedback $u = -Kx$. However, instead of having to determine two weighting matrices that specify $\mathcal{J}$, it would be beneficial to simplify (21) such that there is only one weighting factor. This can be done by taking $Q = \rho C^T C$ and $R = I$. Thus, (21) when simplified becomes

$$\mathcal{J} = \int_0^\infty (\rho y^T y + u^T u) dt \tag{22}$$

where ρ is the weighting factor chosen by the designer. When $\rho \to 0$ it becomes a case of "expensive" control since $\mathcal{J}$ primarily penalizes the use of control energy. Similary, when $\rho \to \infty$ it becomes a case of "cheap" control because an arbitrary control effort may be used by the optimal control law. For purposes of simulation, we will use $\rho = 10$ for determining the gain matrix, K.

In the following Matlab code that has been used to determine K, the matrices A and B have been predefined using (18) and the numerical values in Section 2.2.1.

```
C = eye(4);
R = eye(1);
rho = 10;
Q = rho*C'*C;
K = lqr(A,B,Q,R);
```

Using the above code, we find that,

$$K = \begin{bmatrix} -3.1623 & -14.1162 & -538.8234 & -98.4502 \end{bmatrix} \tag{23}$$

Now that K has been determined, we would like to transcribe the non-linear differential equation model into a Matlab function so that the state variables can be solved using a differential equation solver. Recall that this non-linear model of the cart-stick system was derived earlier in Section 2.1.3. Using a non-linear simulation model over a linear simulation model would ensure that the simulation results are

more accurate. The `ode45` solver in Matlab would be perfect in solving initial value problems for ordinary differential equations in such situations. Accordingly, a Matlab function named `cartStick_stateFeedback` has been coded where the non-linear state equations have been defined. The Matlab code for `cartStick_stateFeedback.m` is given in Section B.3 of Appendix B. Also, the Matlab code for a script file used to solve the non-linear differential equations in `cartStick_stateFeedback` is given in Section B.2 of Appendix B.

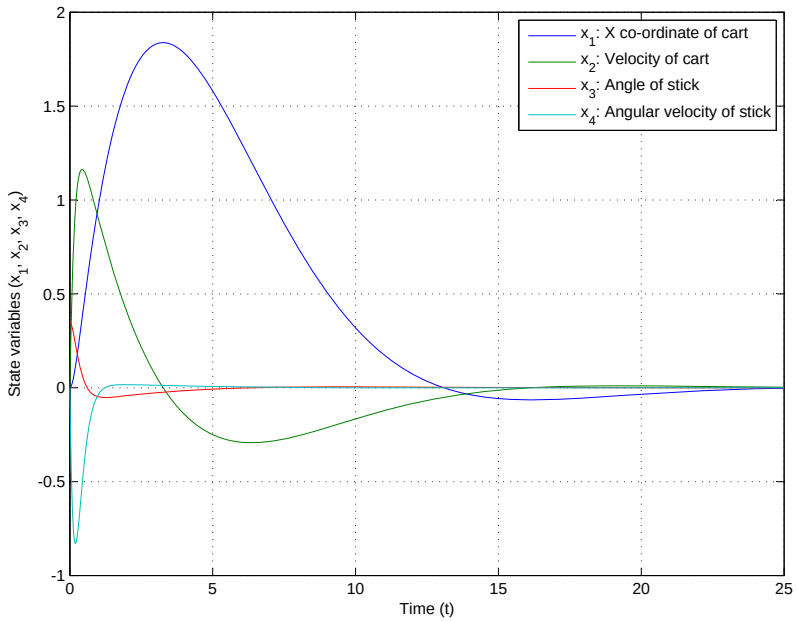

Figure 4: Plot of all state variables versus time for cart-stick system using state-feedback. Simulated initial condition for vertical angle of stick (x_3) is 20° or 0.35 radians. Rest of the state variables are initiated to 0.

It should be noted that the simulation is run for a time span of 25 seconds. The plant initial condition vector has four elements, the state variables x_1 through x_4 and the system control input is the linear force, F. The initial condition used for the vertical angle of the stick is 20° or 0.35 radians. The resulting plot of this simulation showing the four state variables is given in Figure 4. One should also note that SI units have been used in all simulations. As we can see, the system is successfully stabilized with a settling time of approximately 20 seconds. These results will obviously change

for different system parameters and initial conditions.

Another result that might be of interest is the amount of control effort or linear force required to stabilize the cart-stick system using a state-feedback control system with an initial condition stick angle of 20°. Figure 5 shows a plot of the force F required to stabilize the cart-stick system. The unit of F is Newtons. It can be seen that a maximum force of 180.3 N is needed to stabilize the cart-stick system with given system parameters and initial condition.

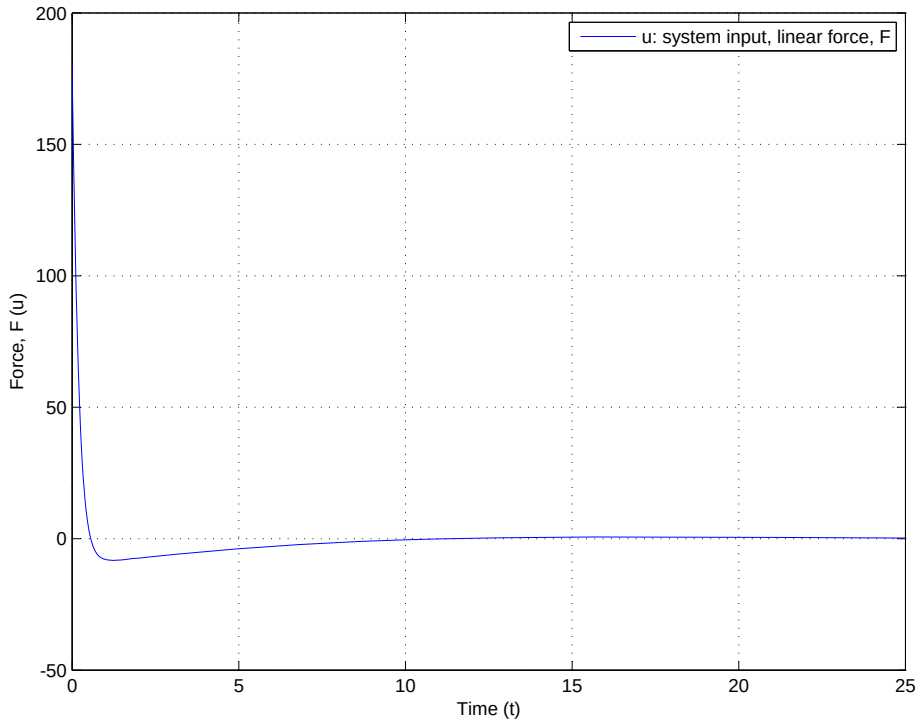

Figure 5: Plot of system input or control effort applied on the cart-stick system using state-feedback. Simulated initial condition for vertical angle of stick (x_3) is 20° or 0.35 radians. Rest of the state variables are initiated to 0.

Having successfully simulated the cart-stick system with an initial condition of 20°, it would now be beneficial to vary the initial condition and see how it affects the simulation results. Thus, the initial condition on the vertical angle of the stick is varied from 35° to 65° in increments of 10°. The simulation results for the same are shown in Figure 6. It can be seen from the simulation results that as the initial condition angle increases, the overshoot in the state variables also increases; such a

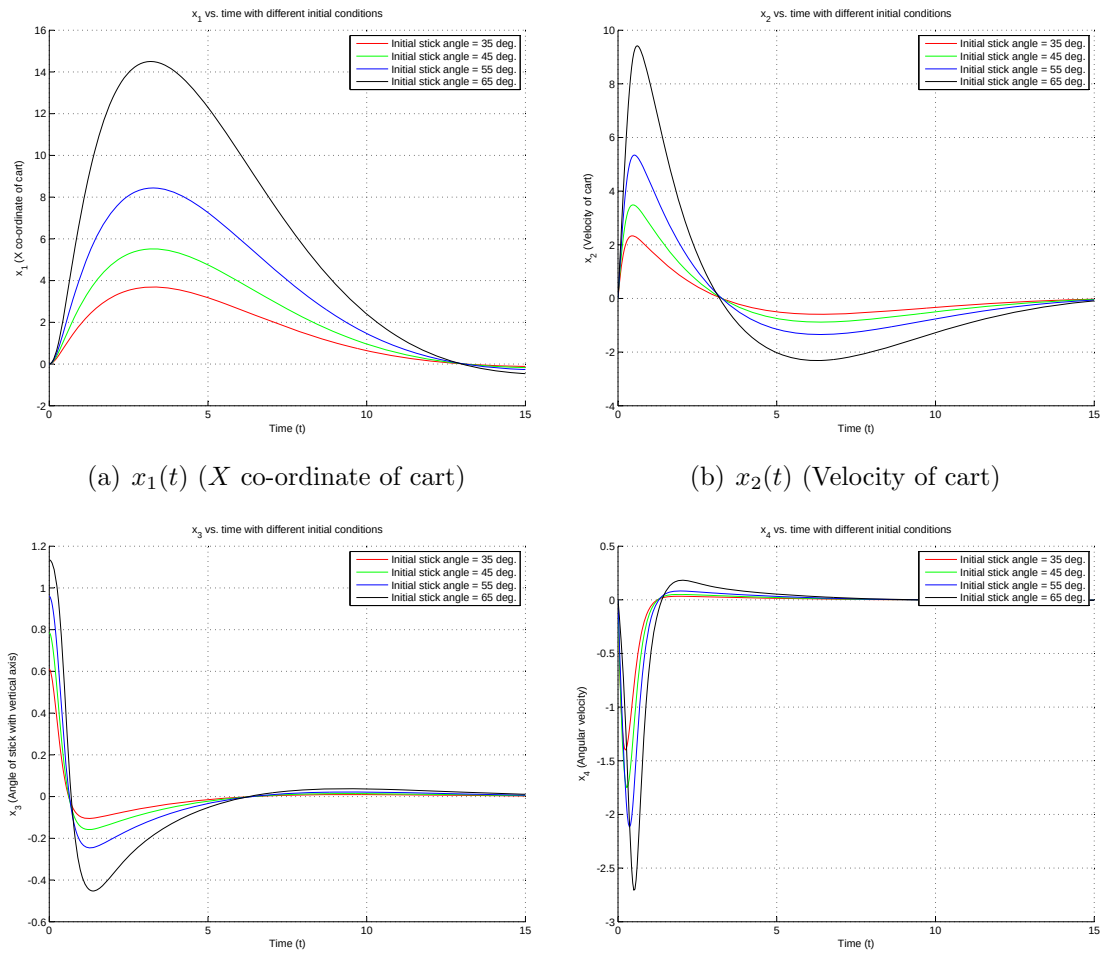

(a) $x_1(t)$ (X co-ordinate of cart)

(b) $x_2(t)$ (Velocity of cart)

(c) $x_3(t)$ (Angle of stick with vertical axis)

(d) $x_4(t)$ (Angular velocity of stick)

Figure 6: Plots of each state variable versus time for various initial conditions. Simulated initial conditions for vertical angle of stick (x_3) are 35°, 45°, 55° and 65°. The unit of angles shown in Figure 6(c) is radians. Rest of the state variables are initiated to 0.

result is expected. It was also found that the system fails to stabilize for any initial condition angle greater than 68°. Thus, for the chosen numerical values of vehicle parameters such as m, M and l, and the control system parameter, ρ, the system can never be stabilized if the initial vertical angle of the stick is greater than 68°. Such a constraint successfully verifies the inherent non-linearities in the plant.

2.2.4 Observability of Cart-Stick System

As discussed earlier, assuming that all state variables are available for measurement is almost never possible. Hence, we need to account for the fact that only a limited number of sensors are available and thus, some state variables will need to be estimated. Recall the continuous-time linear system mentioned in Section 2.2.3 during the discussion of optimal state-feedback design; it is written as

$$\begin{aligned} \dot{x} &= Ax + Bu \\ y &= Cx \end{aligned}$$

where y is the output of the system and C is the output matrix. Usually, y is a vector of sensor measurements and the number of elements in y is equal to the number of sensors being used. After y has been determined by appropriate sensor selection, the output matrix C is determined accordingly. Since observability is a sufficient condition for output-feedback design, our goal here is to find an observable system with the least number of sensors possible.

The system (A, C) is *observable* if, for any $x(0)$, there is a finite time τ such that $x(0)$ can be determined (uniquely) from $u(t)$ and $y(t)$ for $0 \leq t \leq \tau$ [11]. Mathematically, the algebraic observability theorem states that (A, C) is observable if and only if

$$\text{rank} \begin{bmatrix} C \\ CA \\ \vdots \\ CA^{n-1} \end{bmatrix} = n = \dim(x) \tag{24}$$

where the matrix A is from the linear model of the cart-stick system given in (18) and C is determined after sensor selection. Since, there are four state variables in the state-space model of the cart-stick system, $n = \dim(x) = 4$.

For the cart-stick system, there are four relevant sensors that can be used for

measuring required system variables or states. For the first sensor, we can assume that the cart-stick system travels on a fixed track and, consequently, that a linear encoder (optical scanner reading a linear grating mounted beside this track) can be used to precisely measure linear position on the track, $x_1(t)$. For the second sensor, a rotary position encoder can be used to measure $x_3(t)$. Besides these two sensors, a gyroscope can be used to measure $x_4(t)$, and accelerometers could be mounted on the cart to measure the acceleration of the cart. Of these choices, only the position encoders are essentially digital sensors that are practically free from noise, whereas gyroscopes and accelerometers are inherently noisy analog sensors. Hence, we find that

$$y = x_1(t) \quad \text{or} \quad y = x_3(t) \quad \text{or} \quad y = \begin{bmatrix} y_1 \\ y_2 \end{bmatrix} = \begin{bmatrix} x_1(t) \\ x_3(t) \end{bmatrix}$$

Accordingly, using $y = Cx$, for the above options, the matrix C can be

$$\begin{bmatrix} 1 & 0 & 0 & 0 \end{bmatrix} \quad \text{or} \quad \begin{bmatrix} 0 & 0 & 1 & 0 \end{bmatrix} \quad \text{or} \quad \begin{bmatrix} 1 & 0 & 0 & 0 \\ 0 & 0 & 1 & 0 \end{bmatrix}$$

However, using the code given in Section B.1 of Appendix B, it is found that the rank of the observability matrix

$$\begin{bmatrix} C \\ CA \\ CA^2 \\ CA^3 \end{bmatrix}$$

is 4 only when

$$C = \begin{bmatrix} 1 & 0 & 0 & 0 \end{bmatrix} \quad \text{or} \quad C = \begin{bmatrix} 1 & 0 & 0 & 0 \\ 0 & 0 & 1 & 0 \end{bmatrix}$$

Hence, in the interest of using fewest possible sensors, it is determined that the system is observable when $C = \begin{bmatrix} 1 & 0 & 0 & 0 \end{bmatrix}$. This means that only one sensor i.e. a linear encoder will be needed to stabilize the cart-stick system. The next section will

outline the design of an optimal output-feedback control system with the use of an estimator.

2.2.5 Output-Feedback Control System Design

Since the output matrix C has been determined in the previous section, it is now possible to design an output-feedback control system. The design of a general output-feedback control system making the use of an estimator is given by

$$\begin{aligned} \text{Plant:} \quad \dot{x}(t) &= f(x(t), u(t)) \\ \text{Estimator:} \quad \dot{\hat{x}}(t) &= f(\hat{x}(t), u(t)) - H\left[C\hat{x}(t) - y(t)\right] \\ \text{Estimated state-feedback:} \quad u(t) &= -K\hat{x}(t) \end{aligned}$$

where $x_1(t)$, $x_2(t)$, $x_3(t)$, $x_4(t)$ are the actual states and $\hat{x}_1(t)$, $\hat{x}_2(t)$, $\hat{x}_3(t)$ and $\hat{x}_4(t)$ are the corresponding estimated states. Like for the state-feedback system, it should be noted that inherent non-linearities of the cart-stick system are maintained in the simulation model by using non-linear equations for $\dot{x}(t)$ from Section 2.1.3. Also, note that the equations for the estimator in output-feedback design are non-linear. Hence, a non-linear output-feedback system is designed in this case.

Now, the output-feedback control system model given above shows that two gain matrices, K and H need to be determined. As discussed earlier during the modeling of the state-feedback system, one common approach is to assign a set of pole locations and to use the Matlab command `place` to determine the gain matrices. In this situation, since there are two gain matrices, two instances of `place` will need to be used. However, once again, the gain matrices determined by manually assigning pole locations provide satisfactory control, not optimal control.

Analogous to the LQR design technique used in state-feedback design, the LTR technique is widely used for designing output-feedback systems with an estimator. As shown by [9], the introduction of an estimator in a state-feedback controller loop may adversely affect the stability robustness properties of the system. This means that the

phase margin and gain margin properties may become arbitrarily poor. However, it is possible to modify the estimator design so as to try to "recover" the LQR stability robustness properties to some extent and this process is called *loop transfer recovery* [8]. Thus, the central idea behind the LTR technique is to redesign the estimator in such a way as to shape the loop gain properties to approximate those of LQR.

There are design trade-offs associated with the LTR design problem and since it is approximated to an LQR problem, there is a price to be paid for this improvement in stability robustness. As a result, a control system designed using the LTR technique may require more control effort or have worse measures of transient response and sensor noise sensitivity compared to it's LQR counterpart. More details of this discussion are given in [8]. To formulate the LTR problem, consider the continuous-time linear system given by

$$\begin{aligned} \dot{x} &= Ax + Bu + w \\ y &= Cx + v \end{aligned}$$

where w and v are uncorrelated zero-mean white gaussian process and sensor noise with covariance matrices $R_w \geq 0$ and $R_v \geq 0$. These noise parameters, R_w and R_v can be treated as desgin "knobs" to manipulate the design trade-offs. However, instead of having to manipulate two design "knobs", it would be beneficial to have just one design parameter. This can be done by choosing $R_w = \Gamma\Gamma^T$, $R_v = I$ and $\Gamma = qB$, where q is a scalar design parameter [8]. It has been shown that as q becomes large or $q \to \infty$, the degree of recovery can be arbitrarily good [10]. However, this is valid only for minimum-phase systems i.e. systems with zeros in the LHP. It is easy to show that the zeros of this plant with $y = x_1$ as output are at $s = \pm\sqrt{g/l}$. Since, the zeros of our plant are not all in the LHP, the degree of recovery can't be guaranteed. Nonetheless, to systematize the determination of H and for the purposes of simulation, we will use $q = 1000$ for determining the gain matrix, H. To be consistent with the weighting

factor, ρ used in state-feedback, the gain matrix, K will be determined using the same value i.e. $\rho = 10$.

Once more, in the following Matlab code that has been used to determine K and H, the matrices A and B have been predefined using (18) and the numerical values in Section 2.2.1. It should be noted that though K is determined using the Matlab command `lqr`, H is determined using `lqe` or *linear quadratic estimation*.

```
C = eye(4);
R = eye(1);
rho = 10;
Q = rho*(C')*C;
K = lqr(A,B,Q,R);

C = [1 0 0 0];
q = 1000;
gamma = q*B;
Rw = gamma*gamma';
Rv = eye(1);
H = lqe(A,eye(4),C,Rw,Rv);
```

Using the above code, we find that,

$$K = \begin{bmatrix} -3.1623 & -14.1162 & -538.8234 & -98.4502 \end{bmatrix} \tag{25}$$

$$H = \begin{bmatrix} 20.3952 \\ 207.981 \\ -559.392 \\ -3099.77 \end{bmatrix} \tag{26}$$

Now that K and H have been determined, we would like to transcribe the non-linear differential equation model of the output-feedback control system into a Matlab function so that the state variables can be solved using a differential equation solver. Recall once more that this non-linear model of the cart-stick system was derived earlier in Section 2.1.3. Accordingly, a Matlab function named `cartStick_outputFeedback` has been coded where the non-linear model has been defined. The Matlab code for

`cartStick_outputFeedback.m` is given in Section B.4 of Appendix B. The script file given in Section B.2 of Appendix B can be used to solve the differential equations in `cartStick_outputFeedback`.

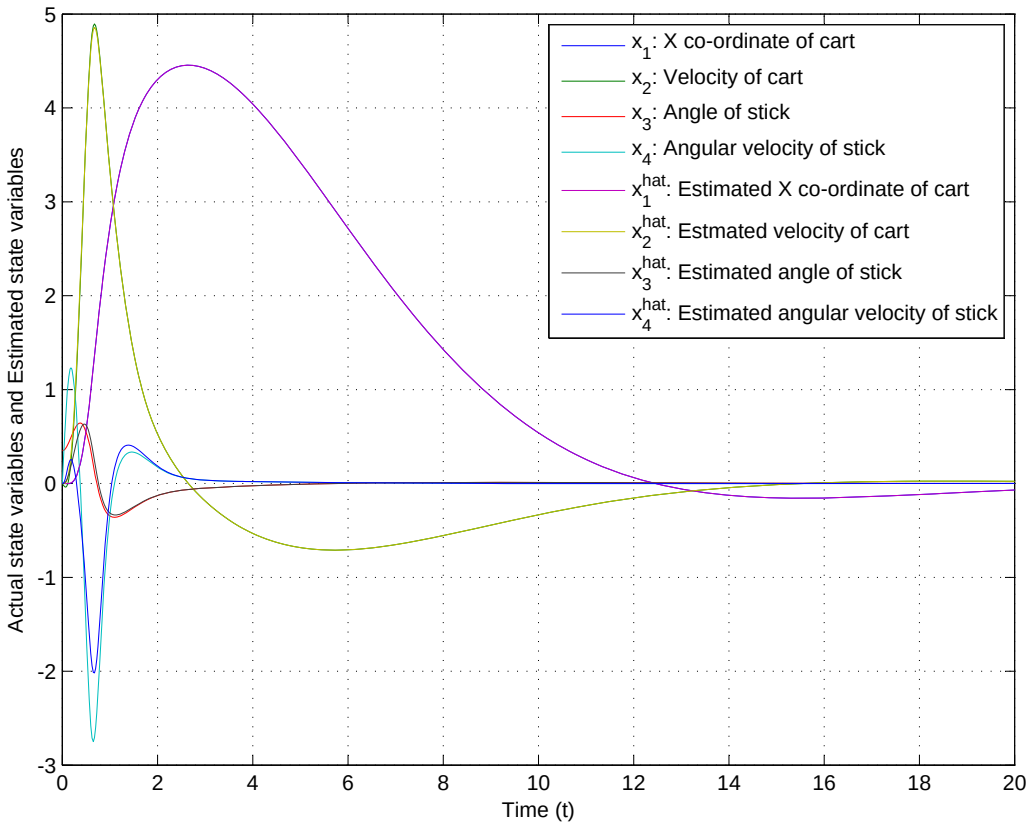

Figure 7: Plot of all actual and estimated state variables versus time for cart-stick system using output-feedback design. Simulated initial condition for vertical angle of stick (x_3) is 20° or 0.35 radians. Rest of the actual state variables and all estimated state variables are initiated to 0.

It should be noted that the simulation is run for a time span of 20 seconds. The resulting plot of this simulation showing the actual and estimated state variables is given in Figure 7. One can see that the estimated states closely follow the actual states and the difference between the actual and estimated states decreases as time elapses. To remain consistent with state-feedback simulations, the initial condition used for the vertical angle of the stick, x_3 is 20° or 0.35 radians. All estimated state variables are initiated to 0. The system is successfully stabilized with a settling time

of approximately 13 seconds. These results will obviously change for different system parameters and initial condition.

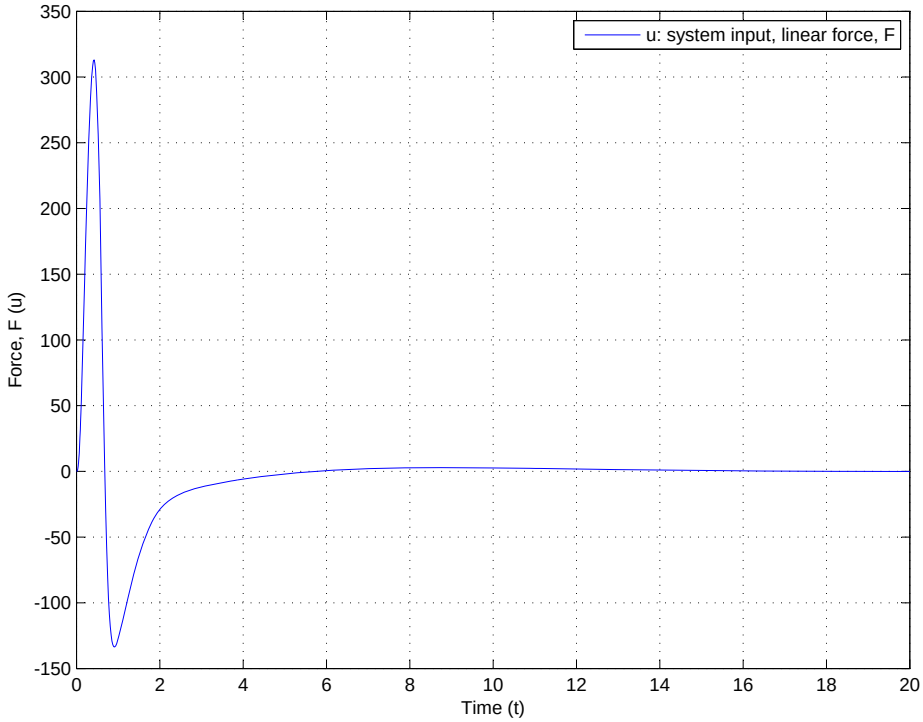

Figure 8: Plot of system input or control effort applied on the cart-stick system using output-feedback design. Simulated initial condition for vertical angle of stick (x_3) is 20° or 0.35 radians. Rest of the state variables are initiated to 0.

As done for state-feedback, another result that might be of interest is the amount of control effort or linear force required to stabilize the cart-stick system with an initial condition stick angle of 20°. Figure 8 shows a plot of the force F required to stabilize the cart-stick system. The unit of F is Newtons. It can be seen that a maximum force of 313 N is needed to stabilize the cart-stick system with given system parameters and initial condition. The initial condition i.e. the vertical angle of the stick can be varied to see its effect on the transient response. Increasing the initial vertical angle would clearly require more control effort. It was also noted that, for the chosen numerical values of vehicle parameters such as m, M and l, and control system parameters such as ρ and q, the system can never be stabilized if the initial

vertical angle of the stick is greater than 26°. Such a constraint again successfully verifies the inherent non-linearities in the plant.

A comparison of the control effort required in a state-feedback control system and an output-feedback control system will be done while discussing the conclusions in Chapter 4. As discussed earlier, it is expected that the LTR design technique degrades transient performance because it is approximated to an LQR design and not all state variable measurements are available for feedback.

Since we have now successfully modeled and simulated the cart-stick system, it is time to move on to the wheeled inverted pendulum system. The same methodology of dynamic modeling and control system design used in the cart-stick system will be followed for the wheeled inverted pendulum system.

CHAPTER III

WHEELED INVERTED PENDULUM SYSTEM

As described earlier, a wheeled inverted pendulum system is a body above two wheels with no balancing support or it's simply a vehicle that balances itself on two coaxial wheels. An illustrative 3D model of the wheeled inverted pendulum system is shown in Figure 2. As it can be seen from this figure, the system has three degrees of freedom i.e. about the X, Y and Z axis. The rotation around the lateral axis (Z) is known as *pitch* and the rotation around the vertical axis (Y) is known as *yaw*. These angles are illustrated specifically for the wheeled inverted pendulum system in Figure 2 and in a more general sense in Figure 9.

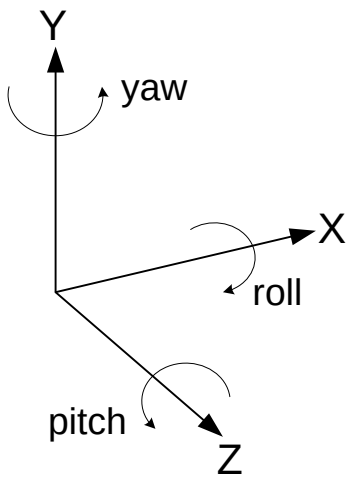

Figure 9: Yaw, pitch and roll angles for a general XYZ co-ordinate system.

Following a similar methodology to the cart-stick system, the first step in designing a control system for the wheeled inverted pendulum system is to derive the equations of motion. This chapter will outline the dynamic modeling of the wheeled inverted pendulum system and the design of controllers for the same. The dynamic modeling will include deriving the equations of motion using the Newtonian and

Lagrangian methods, assigning appropriate state space variables, determining the non-linear state-space model, and deriving the approximate linear model of the non-linear state-space model. The control system design will include the determination of controllability and observability, state-feedback design and output-feedback design. Also, recall that simplifications such as using a fictitious linear force actuator and point mass were introduced during the modeling of the cart-stick system. However, these simplifications will be removed for the wheeled inverted pendulum system by considering a distributed mass for the chassis and introducing wheel dynamics.

3.1 Dynamic Modeling of the Wheeled Inverted Pendulum System

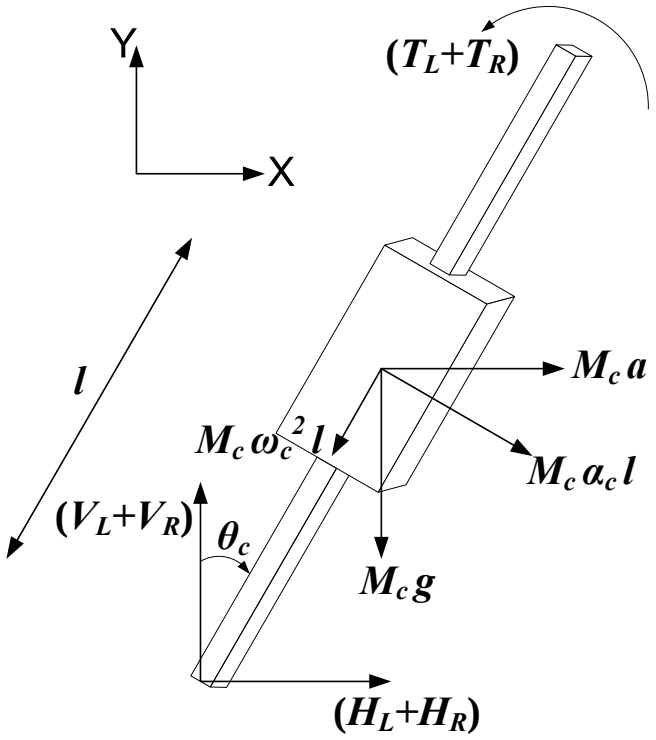

Figure 10: Schematic of the chassis of the wheeled inverted pendulum system with all relevant forces and accelerations labeled. Note that in this figure, $\alpha_c = \ddot{\theta}_c$, $\omega_c = \dot{\theta}_c$ and $a = \ddot{x}$.

As done for the cart-stick system previously, the modeling of the wheeled inverted pendulum system will be done using two approaches: Newtonian and Lagrangian. It

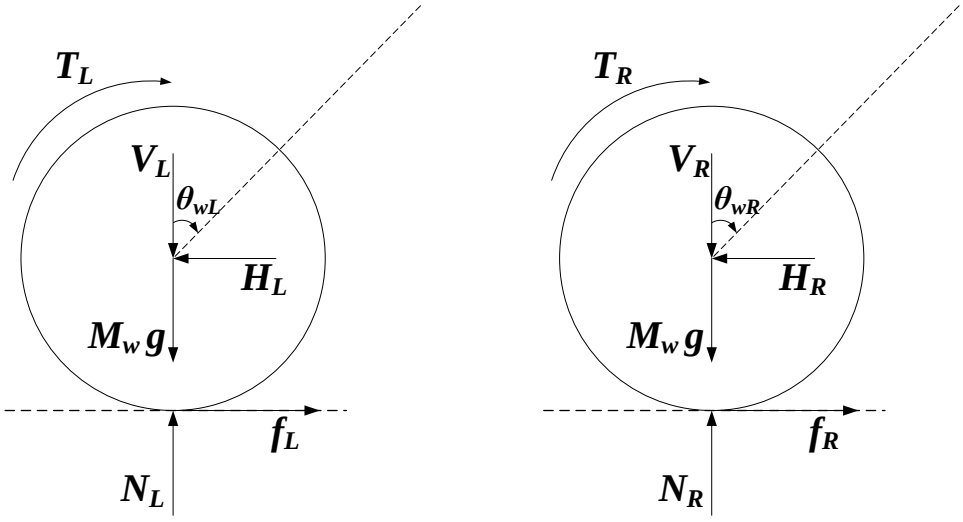

(a) Left wheel (b) Right wheel

Figure 11: Schematics of the left and right wheels of the wheeled inverted pendulum system with all relevant forces and accelerations labeled.

can be verified that the equations obtained from both methods are exactly the same. Thus, deriving the equations of motion from two methods warrants the validity of these equations. It is assumed for both approaches that the right-hand side direction is the $+x$ direction, the upward direction is the $+y$ direction and a clockwise sense is a $+ve$ rotation. Schematic diagrams or free body diagrams of the wheeled inverted pendulum system are shown in Figures 10 and 11. The dynamic modeling of the wheeled inverted pendulum system is done assuming no wheel slip. A list of variables used in the dynamic modeling of the wheeled inverted pendulum system is given in Section A.2 of Appendix A.

3.1.1 Newtonian Approach

Applying $\sum F = Ma$ and $\sum \tau = I\alpha$ on the left wheel, we get the following two equations, respectively

$$M_w \ddot{x}_L = f_L - H_L$$

$$I_w \ddot{\theta}_{wL} = T_L - r f_L \quad \Rightarrow f_L = \frac{T_L - I_w \ddot{\theta}_{wL}}{r}$$

Now, since $\ddot{x}_L = r\ddot{\theta}_{wL}$, the above equations can be simplified to be written as

$$\ddot{x}_L \left(M_w + \frac{I_w}{r^2} \right) = \frac{T_L}{r} - H_L \tag{27}$$

Similarly, the following equation can be derived for the right wheel

$$\ddot{x}_R \left(M_w + \frac{I_w}{r^2} \right) = \frac{T_R}{r} - H_R \tag{28}$$

A dynamic constraint between the horizontal accelerations of the chassis, the left wheel and the right wheel exists. The equation is given by

$$2\ddot{x} = \ddot{x}_L + \ddot{x}_R \tag{29}$$

Adding (27) and (28), and using the dynamic constraint between accelerations gives

$$2 \left(M_w + \frac{I_w}{r^2} \right) \ddot{x} = \frac{T_L + T_R}{r} - (H_L + H_R) \tag{30}$$

Applying $\sum F = Ma$ on the chassis along the X axis we can write

$$M_c\ddot{x} + M_c l\ddot{\theta}_c \cos\theta_c = (H_L + H_R) + M_c l\dot{\theta}_c^2 \sin\theta_c \tag{31}$$

Adding (30) and (31) to eliminate the internal forces H_L and H_R gives

$$\left(2M_w + \frac{2I_w}{r^2} + M_c \right) \ddot{x} = \frac{T_L + T_R}{r} - M_c l\ddot{\theta}_c \cos\theta_c + M_c l\dot{\theta}_c^2 \sin\theta_c \tag{32}$$

Now, the following equation can be achieved by applying $\sum F = Ma$ in a direction perpendicular the chassis and then multiplying that equation by l on both sides

$$M_c\ddot{x}l\cos\theta_c + M_c l^2\ddot{\theta}_c = (H_L + H_R)l\cos\theta_c + M_c gl\sin\theta_c - (V_L + V_R)l\sin\theta_c$$

$$\Rightarrow -(H_L + H_R)l\cos\theta_c + (V_L + V_R)l\sin\theta_c = M_c gl\sin\theta_c - M_c\ddot{x}l\cos\theta_c - M_c l^2\ddot{\theta}_c \tag{33}$$

Since the external torque applied on the wheels is in the clockwise direction, the same torque will be applied on the chassis in the opposite direction (i.e. anti-clockwise). Applying $\sum \tau = I\alpha$ on the chassis gives

$$I_c\ddot{\theta}_c = -(T_L + T_R) - (H_L + H_R)l\cos\theta_c + (V_L + V_R)l\sin\theta_c \tag{34}$$

Equations (33) and (34) can be simplified further to eliminate the internal forces as

$$I_c\ddot{\theta}_c = -(T_L + T_R) + M_c g l \sin\theta_c - M_c \ddot{x} l \cos\theta_c - M_c l^2 \ddot{\theta}_c$$

$$\Rightarrow \ddot{\theta}_c(I_c + M_c l^2) = -(T_L + T_R) + M_c g l \sin\theta_c - M_c \ddot{x} l \cos\theta_c \tag{35}$$

Now, considering the rotational motion of the chassis about the Y axis, and applying the $\sum \tau = I\alpha$ equation, we find that

$$(H_L - H_R)\frac{d}{2} = I_y \ddot{\delta} \quad \Rightarrow (H_L - H_R) = \frac{2I_y\ddot{\delta}}{d} \tag{36}$$

Also, the dynamic constraint of $a_t = \alpha r$ applies for any rotational motion; where a_t is the tangential acceleration, α is the angular acceleration, and r is the radius of curvature for rotational motion. Thus, considering the rotational motion of the two wheels about the vertical Y axis, it follows that

$$\ddot{x}_L = \frac{\ddot{\delta} d}{2} \quad \text{and} \quad -\ddot{x}_R = \frac{\ddot{\delta} d}{2} \tag{37}$$

$$\Rightarrow \ddot{\delta} = \frac{\ddot{x}_L - \ddot{x}_R}{d} \tag{38}$$

Substituting the value of $\ddot{x}_L$ and $\ddot{x}_R$ from (27) and (28) into (38) gives

$$\ddot{\delta} = \frac{\left(\frac{T_L - T_R}{r}\right) - (H_L - H_R)}{d\left(M_w + \frac{I_w}{r^2}\right)} \tag{39}$$

To eliminate H_L and H_R from the above equation, the value of $(H_L - H_R)$ is substituted in the above equation from (36)

$$\ddot{\delta} = \frac{\left(\frac{T_L - T_R}{r}\right) - \left(\frac{2I_y\ddot{\delta}}{d}\right)}{d\left(M_w + \frac{I_w}{r^2}\right)}$$

$$\Rightarrow \ddot{\delta}\left[d\left(M_w + \frac{I_w}{r^2}\right) + \frac{2I_y}{d}\right] = \frac{T_L - T_R}{r}$$

$$\Rightarrow \ddot{\delta}(M_w d^2 r^2 + I_w d^2 + 2I_y r^2) = (T_L - T_R) dr$$

$$\Rightarrow \ddot{\delta} = \frac{(T_L - T_R)dr}{(M_w d^2 r^2 + I_w d^2 + 2I_y r^2)} \tag{40}$$

Equations (32), (35) and (40) are sufficient to describe the dynamics of the wheeled inverted pendulum system.

3.1.2 Lagrangian Approach

The variables used for Lagrangian approach are same as those used for the Newtonian approach. The first step in deriving the equations of motion using the Lagrangian method is to derive the Lagrangian $\mathcal{L}$, which is given by

$$\mathcal{L} = T - V$$

where T and V are the total kinetic and potential energies of the system respectively. For deriving T, the rotational and kinetic energies of the chassis and both wheels need to be considered and for deriving V, the potential energy of the chassis needs to be considered.

Using similar procedure as used in Section 2.1.2 for the cart-stick system, the translational kinetic energy of the chassis can be derived to be

$$\frac{1}{2}M_c[(\dot{x} + l\dot{\theta}_c \cos\theta_c)^2 + (-l\dot{\theta}_c \sin\theta_c)^2] = \frac{1}{2}M_c[\dot{x}^2 + 2\dot{x}l\dot{\theta}_c \cos\theta_c + l^2\dot{\theta}_c^2]$$

The rotational kinetic energy of the chassis is $\frac{1}{2}I_c\dot{\theta}_c^2$. The translational kinetic energies of the left and right wheels are $\frac{1}{2}M_w\dot{x}_L^2$ and $\frac{1}{2}M_w\dot{x}_R^2$ respectively. The rotational kinetic energies of the left and right wheels are $\frac{1}{2}I_w\dot{\theta}_{wL}^2$ and $\frac{1}{2}I_w\dot{\theta}_{wR}^2$ respectively. However, since $\ddot{x}_L = r\ddot{\theta}_{wL}$ and $\ddot{x}_R = r\ddot{\theta}_{wR}$, the rotational kinetic energies of the left and right wheels are $\frac{1}{2}\frac{I_w}{r^2}\dot{x}_L^2$ and $\frac{1}{2}\frac{I_w}{r^2}\dot{x}_R^2$ respectively. The potential energy of the system is $M_c g l \cos\theta_c$. As seen earlier, the Lagrangian is derived by adding all the kinetic energies and subtracting the potential energy as follows

$$\Rightarrow T = \frac{1}{2}M_w\dot{x}_L^2 + \frac{1}{2}M_w\dot{x}_R^2 + \frac{1}{2}\frac{I_w}{r^2}\dot{x}_L^2 + \frac{1}{2}\frac{I_w}{r^2}\dot{x}_R^2 + \frac{1}{2}M_c[\dot{x}^2 + 2\dot{x}l\dot{\theta}_c \cos\theta_c + l^2\dot{\theta}_c^2] + \frac{1}{2}I_c\dot{\theta}_c^2 \tag{41}$$

$$\Rightarrow V = M_c g l \cos\theta_c \tag{42}$$

$$\Rightarrow \mathcal{L} = \frac{1}{2}\left(M_w + \frac{I_w}{r^2}\right)\left(\dot{x}_L^2 + \dot{x}_R^2\right) + \frac{1}{2}M_c\dot{x}^2 + \frac{1}{2}\left(M_c l^2 + I_c\right)\dot{\theta}_c^2 + M_c\dot{x}l\dot{\theta}_c\cos\theta_c - M_c g l\cos\theta_c \tag{43}$$

Now, considering the forces acting on the left wheel and its free body diagram shown in Figure 11(a), the forces that can affect $\ddot{x}_L$ are the torque force $\frac{T_L}{r}$ and the reaction force H_L. Hence, the equation of motion for the left wheel is

$$\frac{d}{dt}\frac{\partial \mathcal{L}}{\partial \dot{x}_L} - \frac{\partial \mathcal{L}}{\partial x_L} = \frac{T_L}{r} - H_L \quad \Rightarrow \quad \left(M_w + \frac{I_w}{r^2}\right)\ddot{x}_L = \frac{T_L}{r} - H_L \tag{44}$$

Similarly, the equation of motion for the right wheel is

$$\frac{d}{dt}\frac{\partial \mathcal{L}}{\partial \dot{x}_R} - \frac{\partial \mathcal{L}}{\partial x_R} = \frac{T_R}{r} - H_R \quad \Rightarrow \quad \left(M_w + \frac{I_w}{r^2}\right)\ddot{x}_R = \frac{T_R}{r} - H_R \tag{45}$$

Adding (44) and (45), and recalling the dynamic constraint $2\ddot{x} = \ddot{x}_L + \ddot{x}_R$ gives

$$2\left(M_w + \frac{I_w}{r^2}\right)\ddot{x} = \frac{T_L + T_R}{r} - (H_L + H_R) \tag{46}$$

The only forces driving the chassis in the X direction are H_L and H_R. Hence, the equation of motion for the chassis is

$$\frac{d}{dt}\frac{\partial \mathcal{L}}{\partial \dot{x}} - \frac{\partial \mathcal{L}}{\partial x} = H_L + H_R$$

$$\Rightarrow M_c\ddot{x} + M_c l\ddot{\theta}_c\cos\theta_c - M_c l\dot{\theta}_c^2\sin\theta_c = H_L + H_R \tag{47}$$

Adding (46) and (47) to eliminate the internal forces H_L and H_R, we find

$$\left(2M_w + \frac{2I_w}{r^2} + M_c\right)\ddot{x} = \frac{T_L + T_R}{r} - M_c l\ddot{\theta}_c\cos\theta_c + M_c l\dot{\theta}_c^2\sin\theta_c \tag{48}$$

Now, the directions of θ_c and the torques T_L and T_R acting on the chassis are opposite in nature. The total torque acting on the chassis is $(T_L + T_R)$. Hence, the equation of motion for the chassis in terms of θ_c is

$$\frac{d}{dt}\frac{\partial \mathcal{L}}{\partial \dot{\theta}_c} - \frac{\partial \mathcal{L}}{\partial \theta_c} = -(T_L + T_R)$$

$$\Rightarrow \frac{d}{dt}\left[(I_c + M_c l^2)\dot{\theta}_c + M_c \dot{x} l \cos\theta_c\right] - \left(-M_c \dot{x} l \dot{\theta}_c \sin\theta_c + M_c g l \sin\theta_c\right) = -(T_L + T_R)$$

$$\Rightarrow \ddot{\theta}_c(I_c + M_c l^2) + M_c \ddot{x} l \cos\theta_c - M_c \dot{x} l \dot{\theta}_c \sin\theta_c + M_c \dot{x} l \dot{\theta}_c \sin\theta_c - M_c g l \sin\theta_c = -(T_L + T_R)$$

$$\Rightarrow \ddot{\theta}_c(I_c + M_c l^2) = -(T_L + T_R) + M_c g l \sin\theta_c - M_c \ddot{x} l \cos\theta_c \tag{49}$$

Thus, it can be seen that (32) and (35) exactly match up with (48) and (49) respectively. This proves the fact that the dynamic modeling of the wheeled inverted pendulum system has been done correctly and the following three equations are sufficient to describe the dynamics of the wheeled inverted pendulum system.

$$\ddot{x}\left(2M_w + \frac{2I_w}{r^2} + M_c\right) = \frac{T_L + T_R}{r} - M_c l \ddot{\theta}_c \cos\theta_c + M_c l \dot{\theta}_c^2 \sin\theta_c \tag{50}$$

$$\ddot{\theta}_c(I_c + M_c l^2) = -(T_L + T_R) + M_c g l \sin\theta_c - M_c \ddot{x} l \cos\theta_c \tag{51}$$

$$\ddot{\delta} = \frac{(T_L - T_R)dr}{(M_w d^2 r^2 + I_w d^2 + 2I_y r^2)} \tag{52}$$

3.1.3 State Assignment and Non-Linear Model

Equations (50) and (51) are not explicitly defined in terms of $\ddot{x}$ and $\ddot{\theta}_c$ and hence need to be solved simultaneously. Solving (50) and (51) simultaneously, we find that

$$\begin{aligned}
\ddot{x} &= \frac{(I_c + M_c l^2)(M_c l \dot{\theta}_c^2 r^2 \sin\theta_c) - M_c^2 l^2 r^2 g \sin\theta_c \cos\theta_c}{(2M_w r^2 + 2I_w + M_c r^2)(I_c + M_c l^2) - M_c^2 l^2 r^2 \cos^2\theta_c} \\
&\quad + \left(\frac{(I_c + M_c l^2)r + M_c l r^2 \cos\theta_c}{(2M_w r^2 + 2I_w + M_c r^2)(I_c + M_c l^2) - M_c^2 l^2 r^2 \cos^2\theta_c}\right)(T_L + T_R) \\
\ddot{\theta}_c &= \frac{(2M_w r^2 + 2I_w + M_c r^2)(M_c g l \sin\theta_c) - M_c^2 l^2 \dot{\theta}_c^2 r^2 \sin\theta_c \cos\theta_c}{(2M_w r^2 + 2I_w + M_c r^2)(I_c + M_c l^2) - M_c^2 l^2 r^2 \cos^2\theta_c} \\
&\quad - \left(\frac{(2M_w r^2 + 2I_w + M_c r^2) + M_c r l \cos\theta_c}{(2M_w r^2 + 2I_w + M_c r^2)(I_c + M_c l^2) - M_c^2 l^2 r^2 \cos^2\theta_c}\right)(T_L + T_R)
\end{aligned}$$

For reasons of simplicity in writing the non-linear equations stated above, the following variables are introduced to represent the respective constant vehicle parameters

$$\mu = (2M_w r^2 + 2I_w + M_c r^2) \tag{53}$$

$$\gamma = (I_c + M_c l^2) \tag{54}$$

$$\beta = (M_w d^2 r^2 + I_w d^2 + 2I_y r^2) \tag{55}$$

$$\psi = (M_c l r) \tag{56}$$

The general form of a state-space model for non-linear systems is given by

$$\dot{x} = f(x, u) \tag{57}$$

where x is a vector of state variables and u is vector of the system control inputs T_L and T_R. The state variable assignment for the wheeled inverted pendulum is done as

$$\begin{aligned}
x_1(t) &= x &&= X \text{ co-ordinate of the chassis} \\
x_2(t) &= \dot{x} &&= \text{Translational velocity of the chassis in the } X \text{ direction} \\
x_3(t) &= \theta_c &&= \text{Pitch angle of the chassis w.r.t the } Y \text{ axis} \\
x_4(t) &= \dot{\theta}_c &&= \text{Pitch angular velocity of the chassis} \\
x_5(t) &= \delta &&= \text{Yaw angle of the chassis w.r.t the } Z \text{ axis} \\
x_6(t) &= \dot{\delta} &&= \text{Yaw angular velocity of the chassis} \\
u_1(t) &= T_L &&= \text{External torque applied on left wheel} \\
u_2(t) &= T_R &&= \text{External torque applied on right wheel}
\end{aligned}$$

Hence, the model equations are written in state space form as

$$\begin{aligned}
\dot{x}_1(t) &= x_2(t) \\
\dot{x}_2(t) &= \frac{\gamma\psi r x_4^2(t)\sin x_3(t) - \psi^2 g \sin x_3(t)\cos x_3(t)}{\mu\gamma - \psi^2\cos^2 x_3(t)} + \left(\frac{\gamma r + \psi r \cos x_3(t)}{\mu\gamma - \psi^2\cos^2 x_3(t)}\right)(u_1(t) + u_2(t)) \\
\dot{x}_3(t) &= x_4(t) \\
\dot{x}_4(t) &= \frac{\mu M_c g l \sin x_3(t) - \psi^2 x_4^2(t)\sin x_3(t)\cos x_3(t)}{\mu\gamma - \psi^2\cos^2 x_3(t)} - \left(\frac{\mu + \psi\cos x_3(t)}{\mu\gamma - \psi^2\cos^2 x_3(t)}\right)(u_1(t) + u_2(t)) \\
\dot{x}_5(t) &= x_6(t) \\
\dot{x}_6(t) &= \frac{dr}{\beta}(u_1(t) - u_2(t))
\end{aligned}$$

3.1.4 Linear Model

Linearization is the process of finding a linear model that approximates a non-linear one. The linear state space model of the aforementioned non-linear model needs to be derived so that tests of controllability and observability can be performed on the model. The first step in deriving the linear approximate model is to determine

the equilibrium points associated with stationary balancing. The equilibrium points are denoted by $(\bar{x}, \bar{u})$ where $\bar{x}$ is a vector of the state variables x_1 through x_6 and $\bar{u}$ is a vector of the torque inputs T_L and T_R. The equilibrium points $(\bar{x}, \bar{u})$ satisfy

$$0 = f(\bar{x}, \bar{u}) \tag{58}$$

where the above equation denotes the non-linear state space model derived in Section 3.1.3. The non-linear model can be rewritten using (58) as

$$\begin{aligned}
0 &= \bar{x}_2 \\
0 &= \frac{\gamma\psi r\bar{x}_4^2 \sin\bar{x}_3 - \psi^2 g \sin\bar{x}_3 \cos\bar{x}_3}{\mu\gamma - \psi^2\cos^2\bar{x}_3} + \left(\frac{\gamma r + \psi r\cos\bar{x}_3}{\mu\gamma - \psi^2\cos^2\bar{x}_3}\right)(\bar{u}_1 + \bar{u}_2) \\
0 &= \bar{x}_4 \\
0 &= \frac{\mu M_c g l \sin\bar{x}_3 - \psi^2\bar{x}_4^2 \sin\bar{x}_3\cos\bar{x}_3}{\mu\gamma - \psi^2\cos^2\bar{x}_3} - \left(\frac{\mu + \psi\cos\bar{x}_3}{\mu\gamma - \psi^2\cos^2\bar{x}_3}\right)(\bar{u}_1 + \bar{u}_2) \\
0 &= \bar{x}_6 \\
0 &= \frac{dr}{\beta}(\bar{u}_1 - \bar{u}_2)
\end{aligned}$$

$$\Rightarrow \quad \bar{x}_1 = \bar{x}_2 = \bar{x}_4 = \bar{x}_5 = \bar{x}_6 = 0 \quad , \quad \bar{u}_1 = \bar{u}_2$$

The remaining equations are

$$-\psi^2 g \sin\bar{x}_3\cos\bar{x}_3 + 2\bar{u}_1(\gamma r + \psi r\cos\bar{x}_3) = 0 \tag{59}$$

$$\mu M_c g l \sin\bar{x}_3 - 2\bar{u}_1(\mu + \psi\cos\bar{x}_3) = 0 \tag{60}$$

Now, there are two unknowns in (59) and (60), namely $\bar{x}_3$ and $\bar{u}_1$ which need to be solved for. Distinct solutions for $\bar{x}_3$ and $\bar{u}_1$ satisfying these equations are

$$\bar{x}_3 = 0 \quad , \quad \bar{u}_1 = 0 \tag{61}$$

$$\bar{x}_3 = \pm\pi \quad , \quad \bar{u}_1 = 0 \tag{62}$$

$$\bar{x}_3 = \pm \arccos\left(\frac{\sqrt{\mu\gamma}}{\psi}\right) \quad , \quad \bar{u}_1 = M_c g l \left[\frac{\sqrt{\mu\gamma} - \mu}{2(\mu - \gamma)}\right] \sqrt{1 - \frac{\mu\gamma}{\psi^2}} \tag{63}$$

$$\bar{x}_3 = \pm \arccos\left(\frac{\sqrt{\mu\gamma}}{\psi}\right) \quad , \quad \bar{u}_1 = M_c g l \left[\frac{\sqrt{\mu\gamma} - \mu}{2(-\mu + \gamma)}\right] \sqrt{1 - \frac{\mu\gamma}{\psi^2}} \tag{64}$$

$$\bar{x}_3 = \pm \arccos\left(-\frac{\sqrt{\mu\gamma}}{\psi}\right) \quad , \quad \bar{u}_1 = M_c g l \left[\frac{-\sqrt{\mu\gamma} - \mu}{2(\mu - \gamma)}\right] \sqrt{1 - \frac{\mu\gamma}{\psi^2}} \tag{65}$$

$$\bar{x}_3 = \pm \arccos\left(-\frac{\sqrt{\mu\gamma}}{\psi}\right) \quad , \quad \bar{u}_1 = M_c g l \left[\frac{-\sqrt{\mu\gamma} - \mu}{2(-\mu + \gamma)}\right] \sqrt{1 - \frac{\mu\gamma}{\psi^2}} \tag{66}$$

However, solution (62) is not a valid equilibrium point for this particular wheeled inverted pendulum system because $\bar{x}_3 = \pm\pi$ would mean that the pitch angle is 180° with respect to the vertical $+y$ direction. Physically, this solution would signify that the chassis of the wheeled inverted pendulum system runs into the ground to achieve equilibrium; however, this is not possible. Hence, solution (62) is not a valid equilibrium point. Also, since the domain of arccos is $[-1, 1]$, solutions (63) to (66) are not valid equilibrium points because the arguments of arccos do not fall in the required domain for these solutions. This domain check can be demonstrated by proving the inequalities

$$-1 \leq \pm\frac{\sqrt{\mu\gamma}}{\psi} \leq 1$$

false. The above inequalities can be reduced to $\psi^2 \geq \mu\gamma$ by simplification. Substituting the values for ψ, μ and γ,

$$M_c^2 l^2 r^2 \geq (2M_w r^2 + 2I_w + M_c r^2)(I_c + M_c l^2)$$

$$\Rightarrow \cancel{M_c^2 l^2 r^2} \geq 2M_w I_c r^2 + 2M_w M_c r^2 l^2 + 2I_w I_c + 2I_w M_c l^2 + M_c I_c r^2 + \cancel{M_c^2 l^2 r^2}$$

Now, the above inequality is not true because every wheeled inverted pendulum parameter in the inequality is a positive, non-zero quantity. The falsification of this inequality proves that the arguments of arccos in the above solutions are not valid. Hence, solutions (63) to (66) are not equilibrium points. It follows that the only

equilibrium point for the wheeled inverted pendulum system is

$$\bar{x} = \begin{bmatrix} \bar{x}_1 \\ \bar{x}_2 \\ \bar{x}_3 \\ \bar{x}_4 \\ \bar{x}_5 \\ \bar{x}_6 \end{bmatrix} = \begin{bmatrix} 0 \\ 0 \\ 0 \\ 0 \\ 0 \\ 0 \end{bmatrix} \quad , \quad \bar{u} = \begin{bmatrix} \bar{u}_1 \\ \bar{u}_2 \end{bmatrix} = \begin{bmatrix} 0 \\ 0 \end{bmatrix} \tag{67}$$

One can compute a linear model that is valid for small signals, for a system with smooth non-linearities and a continuous derivative. Hence, the linear model equations can be derived in the form

$$\dot{x} = Ax + Bu \tag{68}$$

from the general non-linear form

$$\dot{x} = f(x, u)$$

where,

$$A = \begin{bmatrix} \frac{\partial f_1}{\partial x_1} & \cdots & \frac{\partial f_1}{\partial x_6} \\ \vdots & \ddots & \vdots \\ \frac{\partial f_6}{\partial x_1} & \cdots & \frac{\partial f_6}{\partial x_6} \end{bmatrix}_{\bar{x},\bar{u}} \quad \text{and} \quad B = \begin{bmatrix} \frac{\partial f_1}{\partial u_1} & \frac{\partial f_1}{\partial u_2} \\ \vdots & \vdots \\ \frac{\partial f_6}{\partial u_1} & \frac{\partial f_6}{\partial u_2} \end{bmatrix}_{\bar{x},\bar{u}}$$

Solving for A and B, and substituting the values for $\bar{x}$ and $\bar{u}$ from (67), the two matrices can be written as

$$A = \begin{bmatrix} 0 & 1 & 0 & 0 & 0 & 0 \\ 0 & 0 & -\frac{\psi^2 g}{\mu\gamma - \psi^2} & 0 & 0 & 0 \\ 0 & 0 & 0 & 1 & 0 & 0 \\ 0 & 0 & \frac{\mu M_c g l}{\mu\gamma - \psi^2} & 0 & 0 & 0 \\ 0 & 0 & 0 & 0 & 0 & 1 \\ 0 & 0 & 0 & 0 & 0 & 0 \end{bmatrix} \quad \text{and} \quad B = \begin{bmatrix} 0 & 0 \\ \frac{r(\gamma+\psi)}{\mu\gamma - \psi^2} & \frac{r(\gamma+\psi)}{\mu\gamma - \psi^2} \\ 0 & 0 \\ -\frac{(\mu+\psi)}{\mu\gamma - \psi^2} & -\frac{(\mu+\psi)}{\mu\gamma - \psi^2} \\ 0 & 0 \\ \frac{dr}{\beta} & -\frac{dr}{\beta} \end{bmatrix} \tag{69}$$

Hence, the linear model for the wheeled inverted pendulum is given by

$$\dot{x} = \begin{bmatrix} \dot{x_1} \\ \dot{x_2} \\ \dot{x_3} \\ \dot{x_4} \\ \dot{x_5} \\ \dot{x_6} \end{bmatrix} = \begin{bmatrix} 0 & 1 & 0 & 0 & 0 & 0 \\ 0 & 0 & -\frac{\psi^2 g}{\mu\gamma - \psi^2} & 0 & 0 & 0 \\ 0 & 0 & 0 & 1 & 0 & 0 \\ 0 & 0 & \frac{\mu M_c g l}{\mu\gamma - \psi^2} & 0 & 0 & 0 \\ 0 & 0 & 0 & 0 & 0 & 1 \\ 0 & 0 & 0 & 0 & 0 & 0 \end{bmatrix} \begin{bmatrix} x_1 \\ x_2 \\ x_3 \\ x_4 \\ x_5 \\ x_6 \end{bmatrix} + \begin{bmatrix} 0 & 0 \\ \frac{r(\gamma+\psi)}{\mu\gamma - \psi^2} & \frac{r(\gamma+\psi)}{\mu\gamma - \psi^2} \\ 0 & 0 \\ -\frac{(\mu+\psi)}{\mu\gamma - \psi^2} & -\frac{(\mu+\psi)}{\mu\gamma - \psi^2} \\ 0 & 0 \\ \frac{dr}{\beta} & -\frac{dr}{\beta} \end{bmatrix} \begin{bmatrix} T_L \\ T_R \end{bmatrix} \tag{70}$$

3.2 Control System Design

As done for the cart-stick system, the control system for the wheeled inverted pendulum system will be designed using two methods: *state-feedback* and *output-feedback*. To be able to design a *state-feedback* control system, it is sufficient that the system is *controllable*. Similarly, to be able to design an *output-feedback* control system, it is sufficient that the system is *observable*. Thus, we will first determine the controllability of the wheeled inverted pendulum system and then design a state-feedback control system. We will then determine the observability of the wheeled inverted pendulum system and design an output-feedback control system for the same.

3.2.1 Wheeled Inverted Pendulum System Physical Parameters

For simulation purposes, actual values for physical parameters of the wheeled inverted pendulum system need to be used. These values are chosen such that it is possible to actually build the wheeled inverted pendulum system and test the control system on a microcontroller board in real-time. The physical parameter values used

in simulations are

M_w	(mass of each wheel)	=	4	kg
M_c	(mass of the chassis)	=	15	kg
I_w	(moment of inertia of each wheel about the Z axis)	=	0.021	kg·m^2
I_c	(moment of inertia of the chassis about the Z axis)	=	1.684	kg·m^2
I_y	(moment of inertia of the chassis about the Y axis)	=	0.469	kg·m^2
r	(radius of each wheel)	=	0.1	m
l	(distance between center wheels and COM of chassis)	=	0.4	m
d	(distance between the two wheels)	=	0.5	m
g	(acceleration due to gravity)	=	9.81	m/s^2

3.2.2 Controllability of Wheeled Inverted Pendulum System

The system (A, B) is *controllable* if there exists a (piecewise continuous) control signal $u(t)$ that will take the state of the system from any initial state x_i to any desired final state x_f in a finite time interval. Mathematically, the algebraic controllability theorem states that (A, B) is controllable if and only if

$$\text{rank}\begin{bmatrix} B & AB & \cdots & A^{n-1}B \end{bmatrix} = n = \dim(x) \tag{71}$$

where the matrices A and B are from the linear model of the wheeled inverted pendulum system given in (69). Since, there are six state variables in the state-space model of the WIP system, $n = \dim(x) = 6$. The rank of the matrix

$$\begin{bmatrix} B & AB & A^2B & A^3B & A^4B & A^5B \end{bmatrix}$$

is determined to be 6 using the Matlab script given in Section C.1 of Appendix C. Since, the controllability test given in (71) is satisfied, the system is controllable. The wheeled inverted pendulum system can thus be successfully controlled using a state-feedback control system.

3.2.3 State-Feedback Control System Design

Recall from Section 2.2.3 in Chapter 2 that the design of a *state-feedback* control system providing full-state feedback is given by

$$\begin{aligned} \text{Plant:} \quad \dot{x}(t) &= f(x(t), u(t)) \\ \text{State-feedback:} \quad u(t) &= -Kx(t) \end{aligned}$$

where the state-feedback is

$$u = -Kx = -\begin{bmatrix} K_{11} & K_{12} & \cdots & K_{1n} \\ K_{21} & K_{22} & \cdots & K_{2n} \end{bmatrix} \begin{bmatrix} x_1 \\ x_2 \\ \vdots \\ x_n \end{bmatrix}$$

In the above equation, K is said to be the *gain matrix* and for an nth-order system, there will be $2n$ feedback gains, $K_{11}, \ldots, K_{1n}, K_{21}, \ldots, K_{2n}$. For the wheeled inverted pendulum system, $n = 6$ since there are six state variables. It should be noted that inherent non-linearities of the wheeled inverted pendulum system are maintained in the simulation model by using non-linear equations for $\dot{x}(t)$ from Section 3.1.3. However, a linear design model is used to determine the gain matrix, K.

Using the same method that was used for the cart-stick system, it is important to determine the gain matrix, K. Thus, in the following Matlab code that has been used to determine K, $\rho = 10$, and the matrices (A, B) have been predefined using (69) and the numerical values in Section 3.2.1.

```
C = eye(6);
R = eye(2);
rho = 10;
Q = rho*C'*C;
K = lqr(A,B,Q,R);
```

Using the above code, we find that,

$$K = \begin{bmatrix} -2.2361 & -4.4696 & -33.9012 & -8.7036 & 2.2361 & 2.4637 \\ -2.2361 & -4.4696 & -33.9012 & -8.7036 & -2.2361 & -2.4637 \end{bmatrix} \tag{72}$$

Now that K has been determined, similar to the method used for the cart-stick system, we would like to transcribe the non-linear differential equation model into a Matlab function so that the state variables can be solved using a differential equation solver. Recall that this non-linear model of the cart-stick system was derived earlier in Section 3.1.3. The `ode45` solver in Matlab would be perfect in solving initial value problems for ordinary differential equations in such situations. Accordingly, a Matlab function named `wip_stateFeedback` has been coded where the non-linear state-space model has been defined. The Matlab code for `wip_stateFeedback.m` is given in Section C.3 of Appendix C. Similar to the cart-stick system, the Matlab code for a script file used to solve the non-linear differential equations in `wip_stateFeedback` is given in Section C.2 of Appendix C.

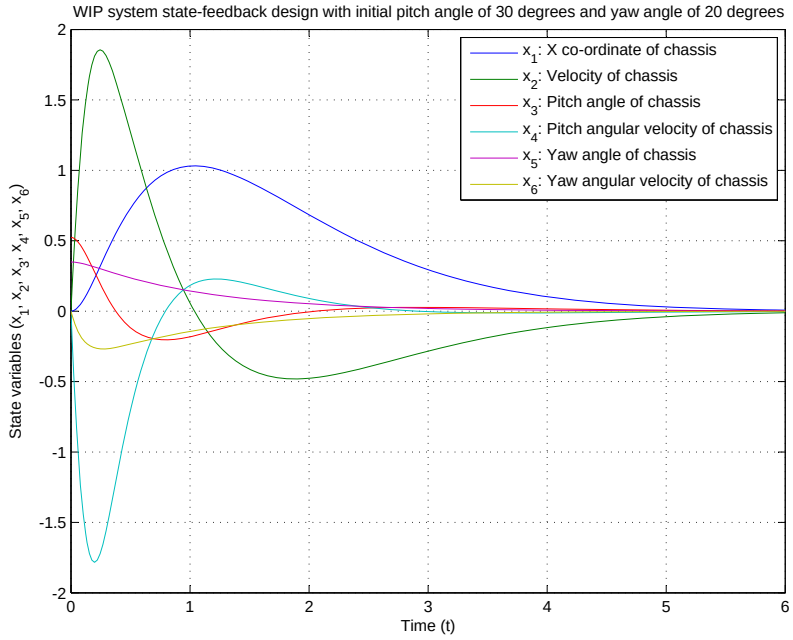

Figure 12: Plot of all state variables versus time for wheeled inverted pendulum system using state-feedback. Simulated initial conditions for pitch angle (x_3) and yaw angle (x_5) of chassis are 30° and 20° respectively. Rest of the state variables are initiated to 0.

It should be noted that the simulation is run for a time span of 6 seconds. The plant initial condition vector has six elements, x_1 through x_6 as expected. The initial

condition used for the pitch or vertical angle of the chassis is 30° or 0.52 radians, whereas the initial condition used for the yaw angle of the chassis is 20° or 0.35 radians. The resulting plot of this simulation showing the six state variables is given in Figure 12. One should also note that SI units have been used in all simulations. As we can see, the system is successfully stabilized with a settling time of approximately 6 seconds. These results will obviously change for different system parameters and initial conditions.

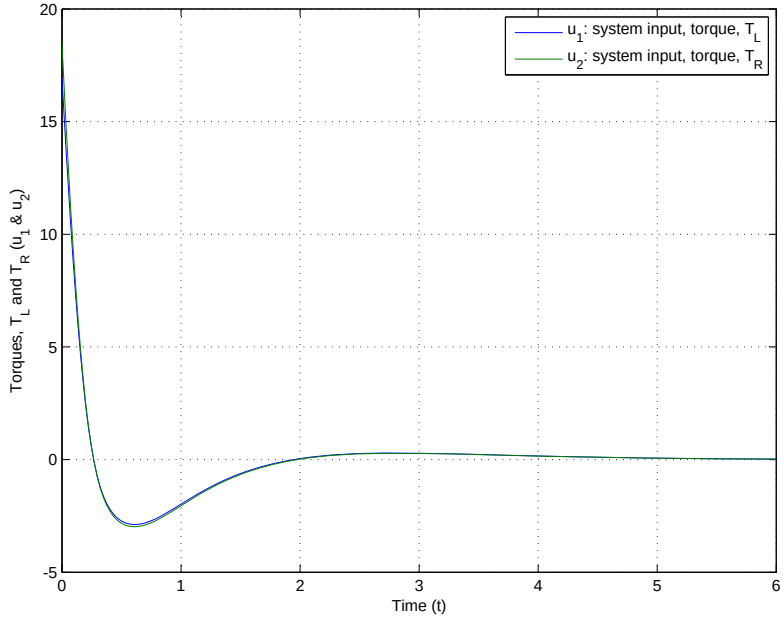

Figure 13: Plot of system inputs, u_1 and u_2 for wheeled inverted pendulum system using state-feedback. Simulated initial conditions for pitch angle (x_3) and yaw angle (x_5) of chassis are 30° and 20° respectively. Rest of the state variables are initiated to 0.

Another result that might be of key interest is the amount of control effort or wheel torques required to stabilize the wheeled inverted pendulum system while using a state-feedback control system with an initial condition pitch angle of 30° and yaw angle of 20°. Figure 13 shows a plot of the torques T_L and T_R required to stabilize the wheeled inverted pendulum system. The unit of torque as shown in this plot is (Newton·meter). It can be seen that, with given system parameters and initial conditions, maximum torques of 16.97 N·m on the left wheel and 18.53 N·m on the

right wheel are needed to stabilize the wheeled inverted pendulum system. One should note that in this situation, both wheels do not require the exact same torque; however, if the yaw angle of chassis is initialized to 0°, both wheels will require the exact same wheel torque in order for the system to be stabilized. This is because the yaw angle of the chassis is associated with turning the wheeled inverted pendulum system and not balancing it; thus if the yaw angle is initiated to 0°, the only task left is to balance the system without having to orient it in the right direction.

The initial conditions of the wheeled inverted pendulum system can be varied to see its effect on the transient response. Increasing the initial pitch angle would clearly require more control effort and degrade transient performance. This phenomenon was illustrated for the cart-stick system in Figure 6. In a wheeled inverted pendulum system with state-feedback, it was also noted that, for the chosen numerical values of vehicle parameters such as masses and moment of inertias, and a control system parameter such as ρ, the system can never be stabilized if the initial pitch angle of the chassis is greater than 77°. Once more, such a constraint successfully verifies that the inherent non-linearities in the wheeled inverted pendulum system are successfully maintained.

3.2.4 Observability of Wheeled Inverted Pendulum System

As discussed earlier during the control system design of the cart-stick system, assuming that all state variables are available for measurement is almost never possible. Hence, we need to account for the fact that only a limited number of sensors are available and thus, some state variables will need to be estimated. Recall that the continuous-time linear system is written as

$$\begin{aligned} \dot{x} &= Ax + Bu \\ y &= Cx \end{aligned}$$

where y is the output of the system and C is the output matrix. Usually, y is a vector of sensor measurements and the number of elements in y is equal to the number of sensors being used. After y has been determined by appropriate sensor selection, the output matrix C is determined accordingly. Since observability is a sufficient condition for output-feedback design, our goal here is to find an observable system with the least number of sensors possible.

The system (A, C) is *observable* if, for any $x(0)$, there is a finite time τ such that $x(0)$ can be determined (uniquely) from $u(t)$ and $y(t)$ for $0 \leq t \leq \tau$. Mathematically, the algebraic observability theorem states that (A, C) is observable if and only if

$$\text{rank} \begin{bmatrix} C \\ CA \\ \vdots \\ CA^{n-1} \end{bmatrix} = n = \dim(x) \tag{73}$$

where the matrix A is from the linear model of the wheeled inverted pendulum system given in (69) and C is determined after sensor selection. Since, there are six state variables in the state-space model of the wheeled inverted pendulum system, $n = \dim(x) = 6$.

Now, the sensor modeling of the wheeled inverted pendulum is a complex problem. Let us assume that we have linear position measurement sensors mounted on each wheel that give us direct measurements of the wheel positions, x_L and x_R. However, it should be kept in mind that such a sensor may not be actually available and thus end up being fictitious. This assumption is being made because a thorough study of the available sensors for the wheeled inverted pendulum system is yet to be done. The remainder of this chapter will assume that such a linear position sensor is available and thus will be used for observability analysis. The second sensor that can be used in the wheeled inverted pendulum system is a gyroscope mounted on the chassis. The gyroscope would give us direct measurements of the pitch angular velocity, $\dot{\theta}_c(t)$. As

a result of these sensor measurement options, we find that

$$y = \begin{bmatrix} y_1 \\ y_2 \end{bmatrix} = \begin{bmatrix} x_L(t) \\ x_R(t) \end{bmatrix} \quad \text{or} \quad y = \begin{bmatrix} y_1 \\ y_2 \\ y_3 \end{bmatrix} = \begin{bmatrix} x_L(t) \\ x_R(t) \\ \dot{\theta}_c(t) \end{bmatrix}$$

However, one should note that though $\dot{\theta}_c$ is one of the state variables, x_L and x_R are not. Hence, to determine the output matrix, C using $y = Cx$, we need to first find a relation between the state variables, and the variables x_L and x_R. Using (29) and (37) from the dynamic modeling of the wheeled inverted pendulum system, we find that

$$x_L = 2x + \frac{d}{2}\delta \quad \text{and} \quad x_R = 2x - \frac{d}{2}\delta$$

but we know from state variable assignment in Section 3.1.3 that $x = x_1$ and $\delta = x_5$. Hence, we can write

$$x_L = 2x_1 + \frac{d}{2}x_5 \quad \text{and} \quad x_R = 2x_1 - \frac{d}{2}x_5 \tag{74}$$

Since a relation has been found between the state variables and the possibly fictitious linear position sensors, the output matrix, C has the following options based on whether or not a gyroscope is used,

$$C = \begin{bmatrix} 2 & 0 & 0 & 0 & \frac{d}{2} & 0 \\ 2 & 0 & 0 & 0 & -\frac{d}{2} & 0 \end{bmatrix} \quad \text{or} \quad C = \begin{bmatrix} 2 & 0 & 0 & 0 & \frac{d}{2} & 0 \\ 2 & 0 & 0 & 0 & -\frac{d}{2} & 0 \\ 0 & 0 & 0 & 1 & 0 & 0 \end{bmatrix} \tag{75}$$

Now, using the code given in Section C.1 of Appendix C, it is found that the rank of the observability matrix

$$\begin{bmatrix} C \\ CA \\ CA^2 \\ CA^3 \\ CA^4 \\ CA^5 \end{bmatrix}$$

is 6 for both options of the output matrix given in (75). Thus, the wheeled inverted pendulum system is observable regardless of whether or not a gyroscope is used. However, we choose to use a gyroscope for better transient performance. Hence,

$$C = \begin{bmatrix} 2 & 0 & 0 & 0 & \frac{d}{2} & 0 \\ 2 & 0 & 0 & 0 & -\frac{d}{2} & 0 \\ 0 & 0 & 0 & 1 & 0 & 0 \end{bmatrix} \tag{76}$$

The next section will outline the design of an optimal output-feedback control system with the use of a non-linear estimator.

3.2.5 Output-Feedback Control System Design

Since the output matrix C has been determined in the previous section, it is now possible to design an output-feedback control system for the wheeled inverted pendulum system. Recall that the design of a general output-feedback control system making the use of an estimator is given by

$$\begin{aligned} \text{Plant:} \quad \dot{x}(t) &= f(x(t), u(t)) \\ \text{Estimator:} \quad \dot{\hat{x}}(t) &= f(\hat{x}(t), u(t)) - H\left[C\hat{x}(t) - y(t)\right] \\ \text{Estimated State-feedback:} \quad u(t) &= -K\hat{x}(t) \end{aligned}$$

where $x_1(t)$, $x_2(t)$, $x_3(t)$, $x_4(t)$, $x_5(t)$ and $x_6(t)$ are the actual states, and $\hat{x}_1(t)$, $\hat{x}_2(t)$, $\hat{x}_3(t)$, $\hat{x}_4(t)$, $\hat{x}_5(t)$ and $\hat{x}_6(t)$ are the corresponding estimated states. Like for the state-feedback system, it should be noted that inherent non-linearities of the cart-stick system are maintained in the simulation model by using non-linear equations for $\dot{x}(t)$ from Section 3.1.3. Also, note that the equations for the estimator in output-feedback design are non-linear. Hence, a non-linear output-feedback system is designed in this case.

It is important to determine the gain matrices, K and H using the same LTR technique discussed while modeling the cart-stick system. Thus, in the following Matlab code that has been used to determine K and H, $\rho = 10$, $q = 1000$, and the

matrices A and B have been predefined using (69) and the numerical values in Section 3.2.1.

```
C = eye(6);
R = eye(2);
rho = 10;
Q = rho*(C')*C;
K = lqr(A,B,Q,R);

C = [2 0 0 0  d/2 0;
     2 0 0 0 -d/2 0;
     0 0 0 1   0  0];
q = 1000;
Gamma = q*B;
Rw = Gamma*Gamma';
Rv = eye(3);
H = lqe(A,eye(6),C,Rw,Rv);
```

Using the above code, we find that,

$$K = \begin{bmatrix} -2.2361 & -4.4696 & -33.9012 & -8.7036 & 2.2361 & 2.4637 \\ -2.2361 & -4.4696 & -33.9012 & -8.7036 & -2.2361 & -2.4637 \end{bmatrix} \tag{77}$$

$$H = \begin{bmatrix} 1.5595 & 1.5595 & -0.5978 \\ 5.2214 & 5.2214 & -955.178 \\ 0.7070 & 0.7070 & 1.0133 \\ -1.1956 & -1.1956 & 1578.66 \\ 102.222 & -102.222 & 0.0000 \\ 2089.864 & -2089.864 & 0.0000 \end{bmatrix} \tag{78}$$

Now that K and H have been determined, as usual we would like to transcribe the non-linear differential equation model of the output-feedback control system into a Matlab function so that the state variables can be solved using a differential equation solver. Accordingly, a Matlab function named `wip_outputFeedback` has been coded where the non-linear model has been defined. The Matlab code for

`wip_outputFeedback.m` is given in Section C.4 of Appendix C. Similar to the cart-stick system, the Matlab code for a script file used to solve the non-linear differential equations in `wip_outputFeedback` is given in Section C.2 of Appendix C.

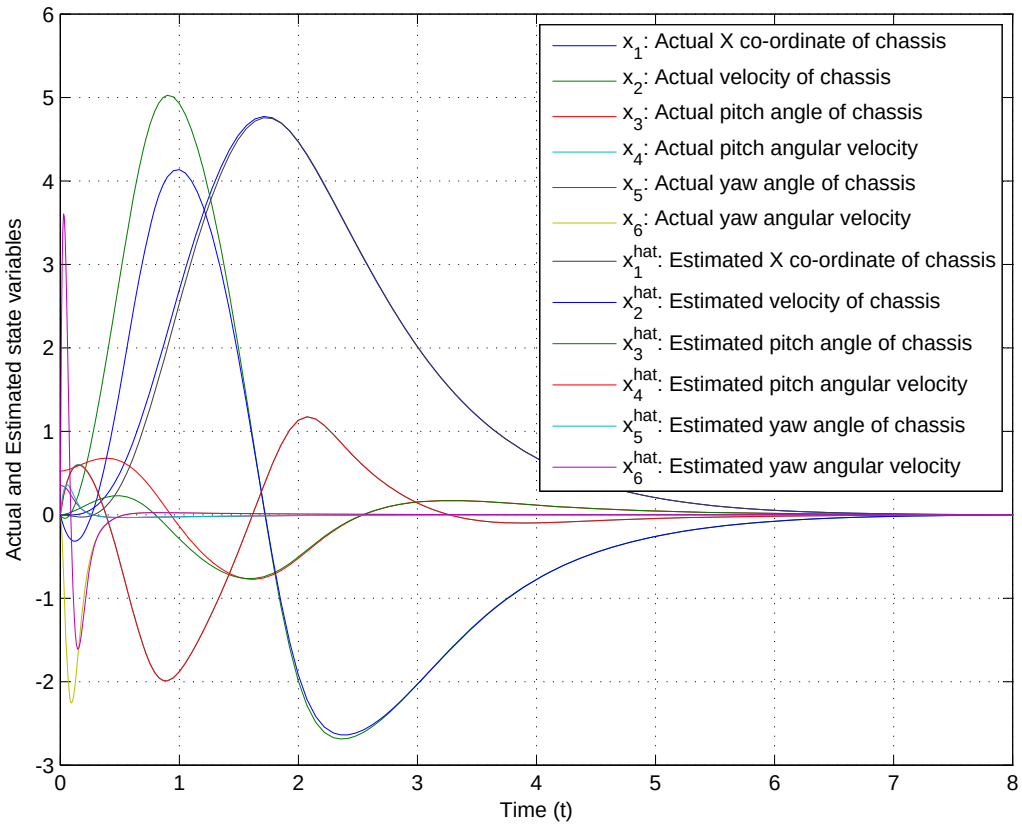

Figure 14: Plot of all actual and estimated state variables versus time for wheeled inverted pendulum system using output-feedback. Simulated initial conditions for pitch angle (x_3) and yaw angle (x_5) of chassis are 30° and 20° respectively. Rest of the state variables are initiated to 0.

It should be noted that the simulation is run for a time span of 8 seconds. The resulting plot of this simulation showing the actual and estimated state variables is given in Figure 14. One can see that the estimated states closely follow the actual states and the difference between the actual and estimated states decreases as time elapses. To remain consistent with state-feedback simulations, the initial conditions used for the pitch angle, x_3 and yaw angle, x_5 of the chassis are 30° and 20° respectively. All estimated state variables are initiated to 0. The system is successfully

stabilized with a settling time of approximately 6 seconds. These results will obviously change for different system parameters and initial conditions. Also, note that another solver called `ode15s` was used instead of `ode45`, because `ode45` was taking a considerable amount of time to solve the differential equations for output-feedback.

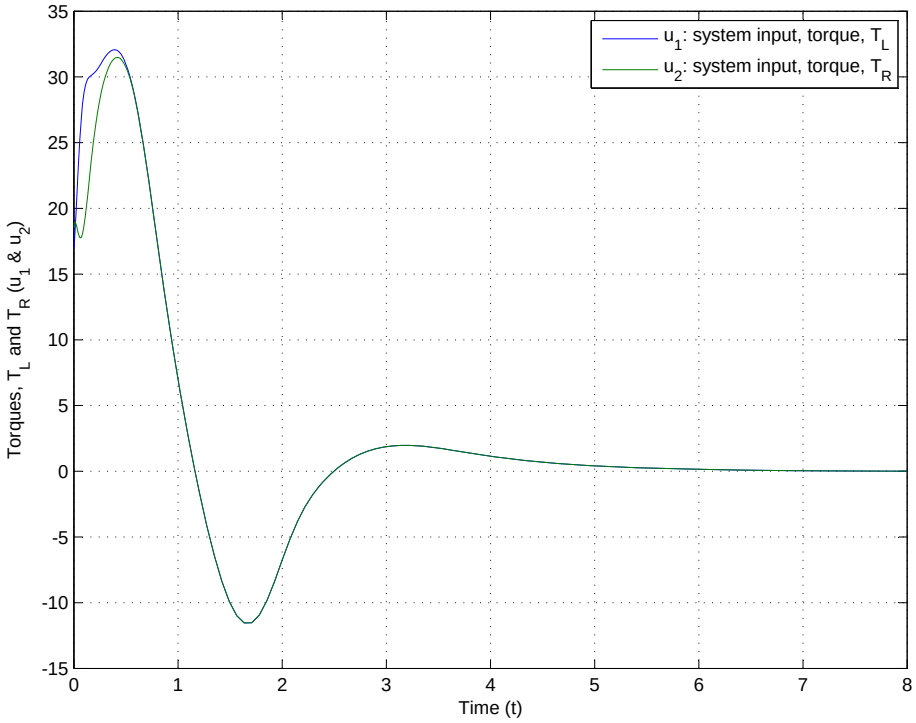

Figure 15: Plot of system inputs, u_1 and u_2 for wheeled inverted pendulum system using output-feedback. Simulated initial conditions for pitch angle (x_3) and yaw angle (x_5) of chassis are 30° and 20° respectively. Rest of the state variables are initiated to 0.

As done for state-feedback, another result that might be of interest is the amount of torque required to stabilize the wheeled inverted pendulum system while using an output-feedback control system with an initial condition pitch angle of 30° and yaw angle of 20°. Figure 15 shows a plot of the torques T_L and T_R required to stabilize the wheeled inverted pendulum system. It can be seen that, with given system parameters and initial conditions, maximum torques of 32.07 N·m on the left wheel and 31.49 N·m on the right wheel are needed to stabilize the wheeled inverted pendulum system. Once more note that both wheels are not given the exact same input torque because

the yaw angle was not initialized to 0°. It was also noted that, in a wheeled inverted pendulum system with output-feedback, for the chosen numerical values of vehicle parameters such as masses and moment of inertias, and control system parameters such as ρ and q, the system can never be stabilized if the initial pitch angle of the chassis is greater than 39°.

A comparison of the control effort required in a state-feedback control system and an output-feedback control system will be done while discussing the conclusions in Chapter 4. As discussed earlier, it is expected that the LTR design technique degrades transient performance because it is approximated to an LQR design and not all state variable measurements are available for feedback.

CHAPTER IV

CONCLUSION

The dynamic modeling and control system design of a complex dynamic system such as the wheeled inverted pendulum system has been successfully performed. Since the wheeled inverted pendulum is a fairly complex system, the cart-stick system was analyzed before analyzing the wheeled inverted pendulum system. The dynamic modeling was done using the Newtonian and Lagrangian approaches to ensure the validity of the equations of motion; the equations achieved through both approaches were exactly the same. The control system design involved simulating state-feedback and output-feedback controllers after determining the controllability and observability of the system. Since state-feedback assumes that all state variables are available for measurement, it became necessary to simulate an output-feedback controller. The assumption that all state variables are available for measurement is not feasible and almost never valid. Owing to the incomplete sensor analysis, it was assumed that the X position of each wheel is available as a measurement. Hence, it was determined that a gyroscope and two sensors that provided linear position measurement of the wheels are sufficient to make the wheeled inverted pendulum system observable. An optimal output-feedback controller was simulated after the output matrix was determined based on appropriate sensor selection.

The most important step in designing the optimal state-feedback and output-feedback controllers was to determine the gain matrices. The LQR (Linear Quadratic Regulator) technique was used to determine the gain matrix, K for the state-feedback controller and the LTR (Loop Transfer Recovery) technique was used to determine the gain matrices, K and H for the output-feedback controller. It is important to

compare the results of the state-feedback and output-feedback designs for the cart-stick and wheeled inverted pendulum systems. These results are compared in the next section.

4.1 State-Feedback versus Output-Feedback

As discussed earlier during the design of an output-feedback controller for the cart-stick system, it was mentioned that the introduction of an estimator in an output-feedback controller loop may adversely affect the stability robustness properties of the system. However, it is possible to modify the estimator design so as to try to "recover" the LQR stability robustness properties of an output-feedback system to some extent; this process is known as Loop Transfer Recovery (LTR). Now, obviously there is a price to be paid for this improvement in stability robustness. The output-feedback system designed using LTR may require more control effort or have worse transient performance compared to that of a state-feedback system. This phenom-

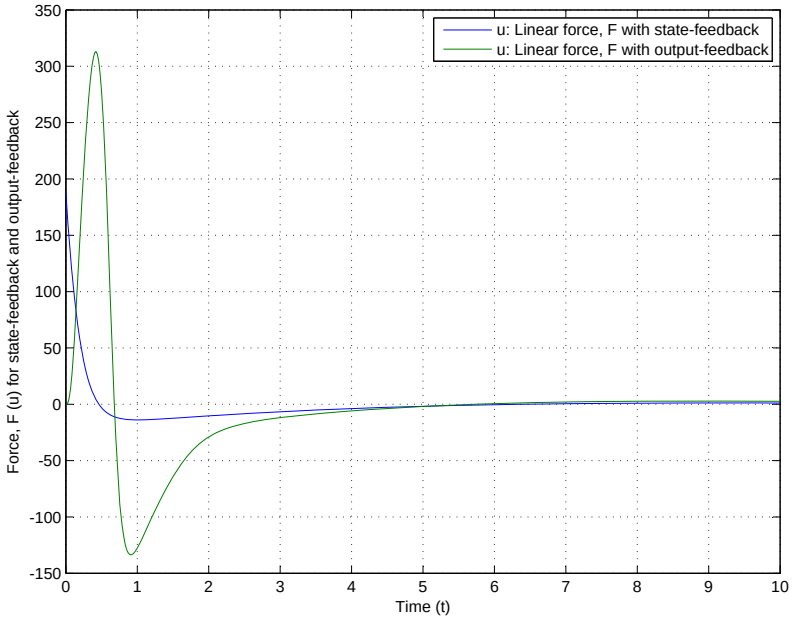

Figure 16: Comparison of system input, F for cart-stick system using state-feedback and output-feedback. Simulated initial condition for vertical angle of stick (x_3) is 20°. Rest of the state variables are initiated to 0.

ena is demonstrated by the simulation results of the cart-stick and wheeled inverted pendulum systems.

Figure 16 compares the system input (linear force, F) of the cart-stick system for state-feedback and output-feedback designs. It is clear from the plot that the control effort required to stabilize the output-feedback system is more than that required by the state-feedback system. A maximum force of 180.3 N is needed to stabilize the cart-stick system using state-feedback, whereas a maximum force of 313 N is needed to stabilize the cart-stick system using output-feedback. An initial vertical stick angle of 20° was used for this simulation.

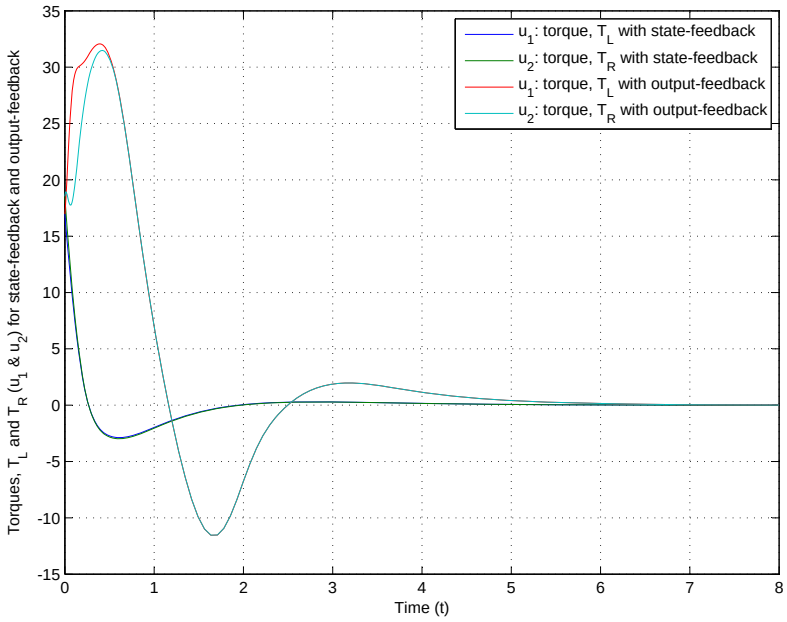

Figure 17: Comparison of system inputs, T_L and T_R for wheeled inverted pendulum system using state-feedback and output-feedback. Simulated initial conditions for pitch angle (x_3) and yaw angle (x_5) of chassis are 30° and 20° respectively. Rest of the state variables are initiated to 0.

Similarly, Figure 17 compares the system inputs (torques, T_L and T_R) of the wheeled inverted pendulum system for state-feedback and output-feedback designs. Once more, it is clear from the plot that the control effort required to stabilize the output-feedback system is more than that required by the state-feedback system. A maximum torque of 18.53 N·m on each wheel is needed to stabilize the wheeled

inverted pendulum system using state-feedback, whereas a maximum torque of 32.07 N·m on each wheel is needed to stabilize the wheeled inverted pendulum system using output-feedback. An initial pitch angle of 30° and yaw angle of 20° was used for this simulation.

Though it is apparent that output-feedback designs using an estimator hamper the performance of a system, it is necessary to consider and prototype output-feedback control systems because all state variables are almost never available for full-state feedback. For example, in the cart-stick system, it was sufficient to measure only one state variable (x_1) instead of all four state variables.

4.2 Future Work

At first, it is necessary to perform accurate sensor analysis and determine the appropriate sensors needed to make the wheeled inverted pendulum system observable. After that, we will augment the controller design with a reference input appropriate for driving and steering the wheeled inverted pendulum, since the current controller only handles stationary balancing of the system. Having done the dynamic modeling and control system simulations for the wheeled inverted pendulum system, the next step is to build the system. The first step towards building the system is to determine the parts and their specifications. The tentative list of parts needed to build the wheeled inverted pendulum system, assuming that some sensors will surely be needed, is

- Microcontroller Board
- Gyroscope
- Optical Wheel Encoders (2)
- Wheels (2)
- Wheel Hubs (2)
- Brush DC Motors (2)

- Gearboxes (2)
- Lithium Ion Battery
- Power Electronics
- Aluminum Body

The specifications for the aluminum body and wheels will be determined based on some of the physical parameters of the system used in the simulations; they are given in Section 3.2.1. The simulation results for the output-feedback control system give us an idea of the torque values required by this wheeled inverted pendulum system. These torque values will then be used to determine the specifications of the motors and gearboxes. The specifications of the gyroscope, wheel encoders and any other required sensors will also be determined accordingly. The specifications for the battery and power electronics will be determined by adding battery dynamics to the simulation model. We have already received a Freescale MPC-555 Microcontroller Board as a donation from Freescale. This board aptly satisfies the needs of the wheeled inverted pendulum system.

After the simulation model is augmented to accommodate driving and battery dynamics, the parts will be ordered and the system will be built in lab. Results from the wheeled inverted pendulum system prototype will be documented as a continuation of this thesis.

APPENDIX A

NOMENCLATURE: LIST OF SYMBOLS

A.1 Cart-Stick System

The following variables have been used to describe the cart-stick system:

m	Mass of the stick (a point mass has been assumed for reasons of simplicity)
M	Mass of the cart
l	Length of the stick
g	Acceleration due to gravity
x	X co-ordinate or position of the cart
v	Translational velocity of the cart
a	Translational acceleration of the cart
P	Vertical relation force between the cart and the stick, acts in the $+y$ direction on the stick and $-y$ direction on the cart
N	Horizontal relation force between the cart and the stick, acts in the $-x$ direction on the stick and $+x$ direction on the cart
F	External force applied on the cart in the $+x$ direction to balance the stick
θ	Vertical angle of the stick
ω	Angular velocity of the stick
α	Angular acceleration of the cart

A.2 Wheeled Inverted Pendulum System

The following variables have been used to describe the wheeled inverted pendulum system:

M_w	Mass of each wheel
I_w	Moment of inertia of each wheel about the Z axis
M_c	Mass of the chassis
I_c	Moment of inertia of the chassis about the Z axis
I_y	Moment of inertia of the chassis about the Y axis
r	Radius of each wheel
l	Distance between the Z axis and the center of gravity of the chassis
d	Distance between the two wheels
g	Acceleration due to gravity
x	X co-ordinate or position of the chassis
x_R	X co-ordinate or position of the right wheel
x_L	X co-ordinate or position of the left wheel
θ_c	Pitch angle for the chassis
θ_{wL}	Rotation angle for the left wheel w.r.t vertical Y axis
θ_{wR}	Rotation angle for the right wheel w.r.t vertical Y axis
δ	Yaw angle for the chassis
V_L	Vertical relation force between the chassis and the left wheel, acts in the $+y$ direction on the chassis and $-y$ direction on the wheel
H_L	Horizontal relation force between the chassis and the left wheel, acts in the $-x$ direction on the wheel and $+x$ direction on the chassis
V_R	Vertical relation force between the chassis and the right wheel, acts in the $+y$ direction on the chassis and $-y$ direction on the wheel

H_R Horizontal relation force between the chassis and the right wheel, acts in the $-x$ direction on the wheel and $+x$ direction on the chassis

f_L Friction acting on the left wheel

f_R Friction acting on the right wheel

T_L External torque applied on the left wheel in the clockwise direction to balance the chassis

T_R External torque applied on the right wheel in the clockwise direction to balance the chassis

APPENDIX B

CART-STICK SYSTEM SIMULATION CODE

B.1 Controllability and Observability

```
% Script to determine Controllability and Observability
% System parameters
syms m M l g

% Linear model
A = [0 1 0 0;
     0 0 -(m*g)/M 0;
     0 0 0 1;
     0 0 ((m+M)*g)/(M*l) 0];

B = [0;
     1/M;
     0;
     -1/(M*l)];

controllabilityRank = rank([B, A*B, A^2*B, A^3*B])

C = [1 0 0 0];
observabilityRank = rank([C; C*A; C*A^2; C*A^3])
```

B.2 Control System Design - Script File

```
clear all
close all
clc

global m M l g
global K H C

%% Define Vehicle Parameters
m = 5;
M = 20;
l = 0.4;
g = 9.81;

A = [0 1 0 0;
```

```
     0 0 -(m*g)/M 0;
     0 0 0 1;
     0 0 ((m+M)*g)/(M*l) 0];

B = [0; 1/M; 0; -1/(M*l)];

%% Determine the gain matrix K
C = eye(4);
R = eye(1);
rho = 1;
Q = rho*(C')*C;
K = lqr(A,B,Q,R);

%% Determine the gain matrix H
C = [1 0 0 0];
q = 1000;
gamma = q*B;
Rw = gamma*gamma';
Rv = eye(1);
H = lqe(A,eye(4),C,Rw,Rv);

Tspan = [0 25];
plantIC = [0;0;20*pi/180;0];
estimatorIC = [0;0;0;0];
options = odeset('RelTol',1e-3);

[t1,x1] = ode45(@cartStick_stateFeedback,Tspan,plantIC);
figure; plot(t1,x1);

uSF = [];
for i = 1:length(t1)
    [xdot1,u1] = cartStick_stateFeedback(t1(i),x1(i,:)');
uSF = [uSF u1];
end

[t2,x2] = ode45(@cartStick_outputFeedback,Tspan,[plantIC;...
            estimatorIC],options);
figure; plot(t2,x2);

uOF = [];
for i = 1:length(t2)
    [xdot2,u2] = cartStick_outputFeedback(t2(i),x2(i,:)');
uOF = [uOF u2];
end
```

```
figure; plot(t1,uSF,t2,uOF);
```

B.3 State-Feedback Control System Design

```
function [xdot,u] = cartStick_stateFeedback(t,x)

global m M l g
global K

u  = -K*x(1:4);

sinf = sin(x(3));
cosf = cos(x(3));

xdot(1) = x(2);
xdot(2) = (m.*l.*x(4).^2.*sinf - m.*g.*sinf.*cosf+ u)./...
            (M + m.*sinf.^2);
xdot(3) = x(4);
xdot(4) = (-m.*l.*x(4).^2.*sinf.*cosf + (M+m).*g.*sinf - ...
            u.*cosf)./(M.*l + m.*l.*sinf.^2);
xdot = xdot';
```

B.4 Output-Feedback Control System Design

```
function [xdot,u] = cartStick_outputFeedback(t,x)

global m M l g
global K H C

xP = x(1:4);
xH = x(5:8);

u  = -K*xH(1:4);
yP = C*xP;
yH = C*xH;

error = yH-yP;
fixError = H*error;

sinfP = sin(xP(3));
cosfP = cos(xP(3));
sinfH = sin(xH(3));
cosfH = cos(xH(3));

xdot(1) = xP(2);
```

```
xdot(2) = (m.*l.*xP(4).^2.*sinfP - m.*g.*sinfP.*cosfP+ u)./...
        (M + m.*sinfP.^2);
xdot(3) = xP(4);
xdot(4) = (-m.*l.*xP(4).^2.*sinfP.*cosfP + (M+m).*g.*sinfP - ...
        u.*cosfP)./(M.*l + m.*l.*sinfP.^2);

xdot(5) = xH(2)-fixError(1);
xdot(6) = ((m.*l.*xH(4).^2.*sinfH - m.*g.*sinfH.*cosfH+ u)./...
        (M + m.*sinfH.^2))-fixError(2);
xdot(7) = xH(4)-fixError(3);
xdot(8) = ((-m.*l.*xH(4).^2.*sinfH.*cosfH + (M+m).*g.*sinfH - ...
        u.*cosfH)./(M.*l + m.*l.*sinfH.^2))-fixError(4);
xdot = xdot';
```

APPENDIX C

WIP SYSTEM SIMULATION CODE

C.1 Controllability and Observability

```
% Script to determine Controllability and Observability of WIP system
% System parameters
syms Mw  Mc Iw Ic Iy r d l g

% Constants in terms of vehicle parameters
mu = (2*Mw*r^2)+(2*Iw)+(Mc*r^2);
gamma = Ic + (Mc*l^2);
beta = (Mw*d^2*r^2)+(Iw*d^2)+(2*Iy*r^2);
psi = Mc*l*r;

% Linear model
A = [0 1 0 0 0 0;
     0 0 -(psi^2*g)/((mu*gamma)- psi^2) 0 0 0;
     0 0 0 1 0 0;
     0 0 (mu*Mc*g*l)/((mu*gamma)- psi^2) 0 0 0;
     0 0 0 0 0 1;
     0 0 0 0 0 0];

B = [0 0;
    r*(gamma+psi)/(mu*gamma - psi^2) r*(gamma+psi)/(mu*gamma - psi^2);
     0 0;
     -(mu+psi)/(mu*gamma - psi^2) -(mu+psi)/(mu*gamma - psi^2);
     0 0;
     (d*r)/beta -(d*r)/beta];

controllabilityRank = rank([B, A*B, A^2*B, A^3*B, A^4*B, A^5*B])

C = [2 0 0 0 d/2 0;
     2 0 0 0 -d/2 0];
observabilityRank1 = rank([C; C*A; C*A^2; C*A^3; C*A^4; C*A^5])

C = [2 0 0 0 d/2 0;
     2 0 0 0 -d/2 0;
     0 0 0 1 0 0];
observabilityRank2 = rank([C; C*A; C*A^2; C*A^3; C*A^4; C*A^5])
```

C.2 Control System Design - Script File

```
clear all
close all
clc

global Mw Mc Iw Ic Iy r d l g mu gamma beta psi
global K H C

%% Define Vehicle Parameters
Mw = 4;     % mass of each wheel
Mc = 15;    % mass of chassis
Iw = 0.021; % moment of inertia of each wheel about Z axis
Ic = 1.684; % moment of inertia of chassis about Z axis
Iy = 0.469; % moment of inertia of chassis about Y axis
r = 0.1;    % radius of each wheel
d = 0.4;    % distance between both wheels
l = 0.5;    % distance between center of both wheels and COM of chassis
g = 9.81;   % acceleration due to gravity

mu = (2*Mw*r^2)+(2*Iw)+(Mc*r^2);
gamma = Ic + (Mc*l^2);
beta = (Mw*d^2*r^2)+(Iw*d^2)+(2*Iy*r^2);
psi = Mc*l*r;

A = [0 1 0 0 0 0;
     0 0 -(psi^2*g)/((mu*gamma)- psi^2) 0 0 0;
     0 0 0 1 0 0;
     0 0 (mu*Mc*g*l)/((mu*gamma)- psi^2) 0 0 0;
     0 0 0 0 0 1;
     0 0 0 0 0 0];

B = [0 0;
    r*(gamma+psi)/(mu*gamma - psi^2) r*(gamma+psi)/(mu*gamma - psi^2);
     0 0;
     -(mu+psi)/(mu*gamma - psi^2) -(mu+psi)/(mu*gamma - psi^2);
     0 0;
     (d*r)/beta -(d*r)/beta];

%% Determine the gain matrix K
C = eye(6);
R = eye(2);
rho = 10;
Q = rho*(C')*C;
K = lqr(A,B,Q,R);
```

```
%% Determine the gain matrix H
C = [2 0 0 0  d/2 0;
     2 0 0 0 -d/2 0;
     0 0 0 1   0  0];
q = 1000;
Gamma = q*B;
Rw = Gamma*Gamma';
Rv = eye(3);
H = lqe(A,eye(6),C,Rw,Rv);

Tspan = [0 10];
plantIC = [0;0;30*pi/180;0;20*pi/180;0];
estimatorIC = [0;0;0;0;0;0];
options = odeset('RelTol',1e-3);

[t1,x1] = ode45(@wip_stateFeedback,Tspan,plantIC,options);
figure; plot(t1,x1);

uSFleft = [];
uSFright = [];
for i = 1:length(t1)
    [xdot1,u1] = wip_stateFeedback(t1(i),x1(i,:)');
    uSFleft = [uSFleft u1(1)]; uSFright = [uSFright u1(2)];
end

[t2,x2] = ode15s(@wip_outputFeedback,Tspan,[plantIC;...
            estimatorIC],options);
figure; plot(t2,x2);

uOFleft = [];
uOFright = [];
for i = 1:length(t2)
    [xdot,u2] = wip_stateFeedback(t2(i),x2(i,:)');
    uOFleft = [uOFleft u2(1)]; uOFright = [uOFright u2(2)];
end

figure; plot(t1,uSFleft,t1,uSFright,t2,uOFleft,t2,uOFright);
```

C.3 State-Feedback Control System Design

```
function [xdot,u] = wip_stateFeedback(t,x)

global Mw Mc Iw Ic Iy r d l g mu gamma beta psi
```

```
global K

u(1) = -K(1,:)*x(1:6);
u(2) = -K(2,:)*x(1:6);

sinf = sin(x(3));
cosf = cos(x(3));

xdot(1) = x(2);
xdot(2) = ((gamma*Mc*l.*x(4).^2.*r^2.*sinf)-(Mc^2*l^2*r^2*g....
            *sinf.*cosf)+(gamma*r + Mc*l*r^2.*cosf).*(u(1)+u(2)))...
            ./((mu.*gamma)-(Mc^2*l^2*r^2.*cosf^2));
xdot(3) = x(4);
xdot(4) = ((mu*Mc*g*l.*sinf)-(Mc^2*l^2*r^2.*x(4).^2.*sinf.*cosf)-...
            (mu + Mc*l*r.*cosf).*(u(1)+u(2)))./((mu.*gamma)-...
            (Mc^2*l^2*r^2.*cosf^2));
xdot(5) = x(6);
xdot(6) = (d*r./beta).*(u(1)-u(2));

xdot = xdot';
```

C.4 Output-Feedback Control System Design

```
function [xdot,u] = wip_outputFeedback(t,x)

global Mw Mc Iw Ic Iy r d l g mu gamma beta psi
global K H C

xP = x(1:6);
xH = x(7:12);

u = -K*xH;
yP = C*xP;
yH = C*xH;

u(1)= -K(1,:)*xH(1:6);
u(2)= -K(2,:)*xH(1:6);

error = yH-yP;
fixError = H*error;

sinfP = sin(xP(3));
cosfP = cos(xP(3));
sinfH = sin(xH(3));
cosfH = cos(xH(3));
```

```
%% Define the plant equations
xdot(1) = xP(2);
xdot(2) = ((gamma*Mc*l.*xP(4).^2.*r^2.*sinfP)-(Mc^2*l^2*r^2*g...
            .*sinfP.*cosfP)+(gamma*r + Mc*l*r^2.*cosfP).*...
            (u(1)+u(2))./((mu.*gamma)-(Mc^2*l^2*r^2.*cosfP^2));
xdot(3) = xP(4);
xdot(4) = ((mu*Mc*g*l.*sinfP)-(Mc^2*l^2*r^2.*xP(4).^2.*sinfP...
            .*cosfP)-(mu + Mc*l*r.*cosfP).*(u(1)+u(2)))./...
            ((mu.*gamma)-(Mc^2*l^2*r^2.*cosfP^2));
xdot(5) = xP(6);
xdot(6) = (d*r./beta).*(u(1)-u(2));

%% Define the estimator equations
xdot(7) = xH(2)-fixError(1);
xdot(8) = (((gamma*Mc*l.*xH(4).^2.*r^2.*sinfH)-(Mc^2*l^2*r^2*g...
            .*sinfH.*cosfH)+(gamma*r + Mc*l*r^2.*cosfH).*...
            (u(1)+u(2)))./((mu.*gamma)-(Mc^2*l^2*r^2.*...
            cosfH^2)))-fixError(2);
xdot(9) = xH(4)-fixError(3);
xdot(10)= (((mu*Mc*g*l.*sinfH)-(Mc^2*l^2*r^2.*xH(4).^2.*...
            sinfH.*cosfH)-(mu + Mc*l*r.*cosfH).*(u(1)+...
            u(2)))./((mu.*gamma)-(Mc^2*l^2*r^2.*cosfH^2)))...
            -fixError(4);
xdot(11)= xH(6)-fixError(5);
xdot(12)= ((d*r./beta).*(u(1)-u(2)))-fixError(6);

xdot = xdot';
```

REFERENCES

[1] Microdynamic Systems Laboratory, Carnegie Mellon University, Dynamically-Stable Mobile Robots in Human Environments. [Online]. Available: http://www.msl.ri.cmu.edu/projects/ballbot [Accessed: July 20, 2009].

[2] N. R. Gans and S. A. Hutchinson, "Visual Servo Velocity and Pose Control of a Wheeled Inverted Pendulum through Partial-Feedback Linearization," in *International Conference on Intelligent Robots and Systems*, Beijing, China, October 9 - 15, 2006, pp. 3823-3828.

[3] F. Grasser, A. DArrigo, S. Colombi, and A. C. Rufer, "JOE: A Mobile, Inverted Pendulum," *IEEE Transactions on Industrial Electronics*, vol. 49, pp. 107-114, February 2002.

[4] S. W. Nawawi, M. N. Ahmad, and J. H. S. Osman, "Real-Time Control of a Two-Wheeled Inverted Pendulum Mobile Robot," *World Academy of Science, Engineering and Technology*, vol. 39, pp. 214-220, 2008.

[5] S. Y. Seo, S. H. Kim, S.-H. Lee, S. H. Han, and H. S. Kim, "Simulation of Attitude Control of a Wheeled Inverted Pendulum," in *International Conference on Control, Automation and Systems*, Coex, Seoul, Korea, Oct. 17-20, 2007.

[6] L. Meirovitch, *Methods of Analytical Dynamics*. Mineola, NY: Dover Publications, 2003.

[7] A. Shimada and N. Hatakeyama, "High-Speed Motion Control of Wheeled Inverted Pendulum Robots," in *International Conference on Mechatronics*, Kumamoto, Japan, 2007.

[8] G. F. Franklin, J. D. Powell, A. Emami-Naeini, *Feedback Control of Dynamic Systems*, 5th ed. Upper Saddle River, NJ: Pearson Prentice Hall, 2006.

[9] J.C. Doyle, "Guaranteed Margins for LQG Regulators," *IEEE Transactions on Automatic Control*, vol. AC-23, pp. 756-777, 1978.

[10] J.C. Doyle and G. Stein, "Robustness with Observers," *IEEE Transactions on Automatic Control*, vol. AC-24, pp. 607-611, 1979.

[11] B. Friedland, *Control System Design: An Introduction to State-Space Methods*, McGraw-Hill, NY, 1986.